Hindawi
Complexity
Volume 2020, Article ID 5891459, 26 pages
https://doi.org/10.1155/2020/5891459

Research Article

Leader-Following Multiple Unmanned Underwater Vehicles Consensus Control under the Fixed and Switching Topologies with Unmeasurable Disturbances

Zheping Yan,[1] Yi Wu ,[1,2] Yibo Liu ,[3] Hongliang Ren ,[2] and Xue Du[1]

[1]*College of Automation, Harbin Engineering University, Harbin 150000, China*
[2]*Department of Biomedical Engineering, National University of Singapore, 119007, Singapore*
[3]*Systems Engineering Research Institute, Beijing 100000, China*

Correspondence should be addressed to Yi Wu; wuyi_ivy@hrbeu.edu.cn

Received 14 November 2019; Revised 5 January 2020; Accepted 7 January 2020; Published 10 February 2020

Academic Editor: Lingzhong Guo

We propose a consensus control strategy for multiple unmanned underwater vehicles (multi-UUVs) with unmeasurable disturbances under the fixed and switching topologies. The current methods presented in the literature mainly solve tracking consensus problems with the disturbances under the time-invariant and time-varying topologies, respectively. In the paper, considering the complex nonlinear and couple model of the UUV, the technique of the feedback linearization is employed to transform the nonlinear UUV model into a second-order integral UUV model. For unmeasurable disturbances consisting of unknown model uncertainties and external disturbance for each UUV, we design the distributed extended state observer (DESO) to estimate the disturbances using the UUV position information relative to its neighbours. Moreover, leader-following multi-UUVs consensus control algorithm that enables all following UUVs to track the leader UUV state information based on the estimation state information from the DESO is proposed for two types of topologies, the fixed and switching topologies. Finally, simulation results are shown to demonstrate the effectiveness of the algorithm proposed in the paper.

1. Introduction

An unmanned underwater vehicle (UUV) is a small underwater vehicle and is capable of propelling itself beneath the water as well as on the surface of water. The UUV is also known as an autonomous underwater vehicle (AUV). The UUV and AUV are autonomous, which means they perform the assigned mission without any human intercession [1]. Recently, the cooperative control of the multi-UUVs has been becoming a hot topic in various applications, including ocean exploration, submarine rescue, minesweeping, and other fields [2–4]. Compared to the individual UUV which has the limited processing power and operational capability [5] to complete a single task, the multi-UUVs as a whole can perform the complex task, thus having more superiority in the harsh ocean environment, such as enhancing reliability and reducing cost. Designing the cooperative control law for the multi-UUVs is a current challenge, which utilizes the UUV location information relative to its neighbours, such that the multi-UUVs agree on the specific quantities of the interest, namely, reaching the consensus control. The development process of the consensus algorithm is reviewed in [6–8], and the algorithm has recently been reached considerably in the context of the cooperative control for multi-agents systems (MASs) with first-order, second-order, or even high-order dynamics. In [9], the adaptive tracking control method was investigated for a second-order system. For designing the tracking control, a novel distributed estimation scheme was proposed to estimate the relative velocity information which was used to design the tracking control. In order to guarantee consensus tracking being reached, linearly parameterized models were first applied to present unknown disturbances and then designed the decentralized adaptive laws for them. As we know, the

consensus algorithm is more challenging for a high-order multiagent system than first-order and second-order ones. A consensus algorithm of high-order multiagents system with antagonistic interactions and communication noises was investigated in [10], in which a novel stochastic-approximation type protocol is proposed to attenuate communication noises and then a bipartite consensus control with communication noises was analyzed from a new perspective. So far, various multi-UUVs consensus control algorithms also have been investigated. Li and Wang [11] introduced the finite-time position consensus algorithm for the multiple autonomous underwater vehicles (AUVs) and discussed the collision avoidance method through building collision avoidance functions. As we know, the communication mode of the multi-UUVs underwater is mainly based on the acoustic wave that has the restriction on the specified frequency, bandwidth, and limited distance, so the effective communication strategy can contribute to reaching the consensus control for the multi-UUVs. Gao and Guo [12] derived the event-triggered communication strategy, which efficiently decreases the communication burden. Novel communication faults control schemes in the multi-UUVs control system were established for accomplishing the consensus control owing to the unreliable acoustic communication condition in the ocean in [13–15].

In the past few years, the consensus algorithm for the multi-UUVs system has extended to the method of the leader-following consensus control in which the leader UUV can guide the team of following UUVs to perform tasks. In order to reach consensus control, the information state of followers would asymptotically converge to that of the leader agent. In [16], the leader-followers consensus control algorithm for the multi-AUVs was proposed, in which the leader guided the followers along the desired trajectory. The controller for the leader-followers was designed by using mathematical and fuzzy artificial potential functions, so the multi-AUVs not only accomplished asymptotically the consensus control but also avoided obstacles successively. Atta and Subudhi [17] discussed the consensus method according to a directed distance-based leader-follower cooperative control for the multi-AUVs. The algorithm for the constrained distance between the followers that avoid collision efficiently among multi-AUVs was developed. Recently, the consensus control for the multi-UUVs with virtual leader UUV has been discussed. In [18], the virtual UUV leader, which was independent with the followers and sent its information state to the UUV neighbours, was designed to reach the consensus control for a group of heterogeneous UUVs. It is a common consensus control algorithm that the team of the UUVs follows only one leader mentioned above called the centralized structure. However, only one leader is not appropriate for a large number of UUV followers. Therefore, the consensus control for the UUV swarm system with some multileaders has been investigated in [19], in which the consensus control algorithm for a UUV swarm system under unreliable communication conditions underwater was investigated. The UUV swarm system consisted of many subgroups including one leader and some followers. A Lyapunov-Krasovskii functional was proposed to obtain consensus conditions. Some novel leader-following consensus control methods [20–22] were proposed to solve the problem of time-delays for the multi-UUVs in our past research work. The communication topology discussed above is time-invarying communication topology, but the topology is often changing, since the communication link may be unreliable underwater for the multi-UUVs.

As an urgent desire has come up for the high-precision control in the MASs, disturbance attenuation has become increasingly important and much attention has been paid to MASs with disturbance. Event-triggered control for consensus problem in MASs with quantized relative state measurements and external disturbance were investigated in [23]. Two type protocols for the quantized control and the event-triggered control were designed to investigate the bounded consensus of general linear MASs with quantized relative state measurements and nonbounded disturbance in the paper. For tackling the problem of disturbance, a high gain method was proposed to recompense for the effects of the external disturbances. In [24], a robust consensus for fractional MASs with external disturbances was investigated. Analyzing the disturbance rejection properties for both linear and nonlinear systems was through the combination of the tools of Mittag-Leffler stability theory, the inequality techniques and Laplace transform. In view of the consensus algorithm for high-order MASs system, the work [25] investigated the a bipartite consensus problem for a high-order MASs with unknown disturbances and cooperative-competitive interactions, in which linearly parameterized approaches were firstly applied to present the time-varying unknown disturbances, and then distributed adaptive laws were designed for the unknown parameters in the disturbances. The consensus performance of the multi-UUVs is also affected by the unmeasurable disturbances, such as uncertainties, modelling errors, and environmental disturbances. Therefore, solving the multi-UUVs consensus problem with unmeasurable disturbances has been becoming important. Some control strategies have been investigated to compensate for the disturbances. The robust compensation algorithm was proposed to attenuate the disturbance for the multi-AUVs in [26, 27], in which the graph theory and the robust compensation theory were used to reach the multi-AUVs consensus with disturbances. In [28, 29], the disturbance observer which estimated the disturbances to compensate the disturbances was proposed for the multi-AUVs, where the disturbance in each AUV is bounded. However, the disturbance observer is based on both the position state information and the velocity state information from the neighbours to estimate the disturbance. Therefore, it is inappropriate for the multi-UUVs to transmit a large amount of information timely and accurately under unstable communication conditions in the ocean.

The research of nonlinear control theory has been playing an increasingly important role for MASs [9, 25, 30–32] and has also become necessary in the design of the consensus control for the multi-UUVs, including the back stepping-based [33], adaptive-based [34, 35], slide mode-

based [36], and neutral networks-based [37–39] consensus control.

In this paper, a leader-following multi-UUVs consensus algorithm with unmeasurable disturbances under the fixed and switching topologies is discussed. Firstly, we transform the nonlinear UUV model into a second-order linear dynamic model by taking the method of the feedback linearization. The coordinate transformation presents the basic idea with feedback linearization instead of the conventional control techniques proposed by Shojaei and Arefi [40]. Secondly, the leader-following multi-UUVs consensus algorithm with unmeasurable disturbances under the fixed topology and the switching topology is proposed, and the stability of the multi-UUVs system is then analyzed. The main contribution of this paper is summarized as follows:

(1) The leader-following multi-UUVs consensus with disturbances under switching topologies is mainly investigated in this paper. Achieving the multi-UUVs consensus with fixed topology is relatively simple but reaching the leader-following multi-UUVs consensus with changing topology as time is becoming challenging. Meanwhile, the case of the switching topology is more practical underwater due to unreliable and limited communication conditions. Unlike [41], which considered MASs under the fixed topologies in the presence of disturbances, it is not appropriate for multi-UUVs performing tasks in the complex ocean environment.

(2) The DESO based on the relative position state for its neighbours is designed to estimate the lumped disturbance consisting of unknown model uncertainties and external disturbances in a multi-UUVs system under switching topology. Compared to the disturbance observer based on both the position information state and the velocity information state to estimate the lumped disturbance in [29], the DESO proposed in the literature estimates lumped disturbance only through the position state information. This can reduce the communication burden between the multi-UUVs in the unreliable underwater communication condition.

The remaining part of this paper is organized as follows: Section 2 contains some necessary preliminaries and problem formulation. Section 3 discusses the leader-following consensus algorithm with the time-invarying communication topology. Section 4 extends the result investigated in Section 3 to the case of the time-varying communication topology. Section 5 illustrates the simulations to verify the result proposed in the paper. Section 6 gives a brief conclusion.

2. Problem Statement and Preliminaries

2.1. Notation. The following notions are utilized throughout this literature:$\mathbb{R}^{n\times m}$ and $\mathbb{R}^n$ represent the set of $n\times m$ real matrices and $n\times 1$ real vectors, respectively. I_n, 0_n, and $0_{n\times m}$ denote $n\times n$ identity matrix, $n\times n$ zero matrix, and $n\times m$ zero matrix. 1_n shows $n\times 1$ column vector of all ones. $\|\cdot\|$ denotes the Euclidean norm. For a symmetric matrix F, $F>0$ (≥ 0, <0 or ≤ 0) denotes that F is a positive definite matrix (positive semidefinite matrix, negative definite matrix, or negative semidefinite matrix). $\lambda_i(A)$, $i=1,2,\ldots,n$ shows the i-th eigenvalue of a matrix A. $\lambda_{\min}(A)$ and $\lambda_{\max}(A)$ mean the minimum and maximum nonzero eigenvalue of the matrix A, respectively. $\mathrm{diag}(a_1,\ldots,a_n)$ and $\mathrm{diag}(A_1,\ldots,A_n)$ represent a diagonal matrix and a block diagonal matrix. For the multi-UUVs, i shows the index of the UUV in the paper, i.e., $i=1,\ldots,N$. $\otimes$ means the Kronecker product referring to [42]. For any matrix W, X, Y Z, the following arguments associated with the Kronecker product is used in the sequel:

(1) $(W\otimes X)(Y\otimes Z)=WY\otimes XZ$;

(2) $X\otimes(Y+Z)=X\otimes Y+X\otimes Z$;

(3) $(Y\otimes Z)^T=Y^T\otimes Z^T$.

2.2. Graph Theory. For the multi-UUVs system in the paper, one leader UUV labeled as the node 0 and following UUVs labeled as node from 1 to N. We use a graph to represent the communication topology among the multi-UUVs. A graph $G=(V,\varepsilon)$ is denoted as the communication topology for the following UUVs, where $V=\{1,\ldots,N\}$ describes a set of nodes meaning N UUVs and $\varepsilon=\{(i,j)\colon i,j\in V\}\subset V\times V$ shows a set of edges. For the undirected graph, the edge (i,j) means that the i-th UUV and the j-th UUV can receive information from each other. The adjacency matrix $A_G=[a_{ij}]\in\mathbb{R}^{N\times N}$ associates with the graph G where $a_{ij}>0$, if $(i,j)\in\varepsilon$ while $a_{ij}=0$, otherwise. The set of the neighbour of UUV i is described as $N_i=\{j\in V\colon (i,j)\in\varepsilon, j\neq i\}$. Define $L=[l_{ij}]\in\mathbb{R}^{N\times N}$ as th Laplacian matrix where $l_{ii}=\sum_{j=1,j\neq i}^{N}a_{ij}$, $l_{ij}=-a_{ij}$, $i\neq j$, noting $l_{ii}<0$, $i\neq j$, $\sum_{j=1}^{N}l_{ij}=0$, $i=1,\ldots,N$. The subpart of the graph G describes the subgraph which is connected in the graph G. For a set s, $|s|$ denotes the number of the element in the set s. A graph $\overline{G}$ includes the graph G, the node UUV 0, and edges between the leader and the followers. Define the matrix $Q=\mathrm{diag}(q_1,\ldots,q_N)$ where $q_i>0$ means that the leader is a neighbour of UUV i and $q_i=0$ otherwise. Define the structure matrix $F=L+Q$. For more detailed explanation, refer to the literature [42].

2.3. Five Degrees of Freedom UUV Models. The roll motion which is the rotation about the longitudinal axis has less influence on the UUV performance because of the torpedo-like shape of the UUV in [43], so we consider five motion components of the UUV consisting of the surge, sway, heave, pitch, and yaw in this paper (see Table 1).

The nonlinear kinematics and dynamic model of an UUV based on the body-fixed and earth-fixed coordinate system in Figure 1 is

$$\begin{aligned}\dot{\eta}&=J(\eta)\upsilon,\\ M_{RB}\dot{\upsilon}+C_{RB}(\upsilon)\upsilon&=\tau,\end{aligned}\tag{1}$$

where $\eta=[x,y,z,\theta,\psi]^T\in\mathbb{R}^5$ is the state information of the position/Euler angles, and $\upsilon=[u,v,w,q,r]^T\in\mathbb{R}^5$ is the

Table 1: The symbols for an UUV.

	Forces and moments	Linear/angular velocities	Positions/Euler angles
Surge	X	u	x
Sway	Y	v	y
Heave	Z	w	z
Pitch	M	q	θ
Yaw	N	r	ψ

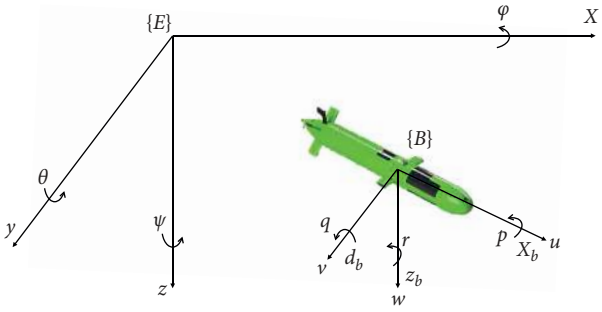

Figure 1: The body-fixed and earth-fixed coordinate systems for an UUV.

state information of velocities for an UUV. $J(\eta)$, M_{RB}, $C_{RB}(\upsilon)$, and τ are the Jacobian matrix, the inertia matrix, Coriolis and centripetal forces, and a vector of generalized forces, respectively. The detailed explanation about terms in (1) is described in the following parts referring to [35].

The representation of the Jacobian matrix $J(\eta)$ is

$$J(\eta) = \operatorname{diag}\left(J_1(\eta), J_2(\eta)\right), \tag{2}$$

where $J_1(\eta) = \begin{bmatrix} \cos\psi\cos\theta & -\sin\psi & \cos\psi\sin\theta \\ \sin\psi\cos\theta & \cos\psi & \sin\psi\sin\theta \\ -\sin\theta & 0 & \cos\theta \end{bmatrix}$ and $J_2(\eta) = \operatorname{diag}(1, 1/\cos\theta)$.

In the paper, it is assumed that the coordinate system locates in the center of gravity so that $[x_g, y_g, z_g] = [0, 0, 0]$ and the center of buoyancy is $[0, 0, z_B]$. Commonly assume that the UUV has homogeneous distribution and xz-plane symmetry such that the products of inertia is $I_{xy} = I_{yx} = I_{xz} = I_{zx} = I_{yz} = I_{zy} = 0$. Under the assumptions mentioned above, the inertia matrix M_{RB} and Coriolis and centripetal forces $C_{RB}(\upsilon)$ in (1) can be represented as follows:

$$M_{RB} = \operatorname{diag}\left(m, m, m, I_y, I_z\right),$$
$$C_{RB}(\upsilon) = \begin{bmatrix} 0 & -mr & mq & 0 & 0 \\ mr & 0 & 0 & 0 & 0 \\ -mq & 0 & 0 & 0 & 0 \\ 0 & 0 & 0 & 0 & 0 \\ 0 & 0 & 0 & 0 & 0 \end{bmatrix}, \tag{3}$$

where m is the mass of the UUV.

For τ in (1), it consists of hydrostatics τ_B, hydrodynamics τ_H, control input τ_R, such as rudders, propellers, and bow thrusters, and disturbances τ_d, then τ is written as

$$\tau = \tau_B + \tau_H + \tau_R + \tau_d. \tag{4}$$

It is common that the neutral UUV would satisfy

$$W = B, \tag{5}$$

where W and B mean the weight of the UUV and buoyancy force, respectively. According to the condition of $W = B$, the center of gravity and buoyancy mentioned above, hydrostatics τ_B can be shown as follows:

$$\tau_B = \left[0, 0, 0, z_B \sin\theta, 0\right]^T. \tag{6}$$

Hydrodynamic forces and moment τ_H in (2) mainly includes added mass τ_{add} and viscous damping τ_{vis}:

$$\tau_H = \tau_{\text{add}} + \tau_{\text{vis}}, \tag{7}$$

where the coefficient of the added mass τ_{add} is shown as follows:

$$M_A = \begin{bmatrix} X_{\dot{u}} & 0 & 0 & 0 & 0 \\ 0 & Y_{\dot{v}} & 0 & 0 & Y_{\dot{r}} \\ 0 & 0 & Z_{\dot{w}} & Z_{\dot{q}} & 0 \\ 0 & 0 & M_{\dot{w}} & M_{\dot{q}} & 0 \\ 0 & N_{\dot{v}} & 0 & 0 & N_{\dot{r}} \end{bmatrix}, \tag{8}$$

and the viscous damping τ_{vis} relating to skin friction, wave drift damping, vortex shedding, and lift/drag in [43]. The viscous damping τ_{vis} can be given as follows:

$$\tau_{vis} = \begin{bmatrix} X_{qq}q^2 + X_{rr}r^2 \\ Y_{qr}qr + Y_{r|r|}r|r| \\ Z_{rr}r^2 + Z_{q|q|}q|q| \\ M_{q|q|}q|q| + M_{rr}r^2 \\ N_{r|r|}r|r| + N_{qr}qr \end{bmatrix} + \begin{bmatrix} X_{vr}vr + X_{wq}wq \\ Y_{ur}ur + Y_{vq}vq + Y_{wr}wr + Y_{v|r|}\dfrac{v}{|v|}\sqrt{v^2+w^2}\,|r| \\ Z_{uq}uq + Z_{vr}vr + Z_{w|q|}\dfrac{w}{|w|}\sqrt{v^2+w^2}\,|q| \\ M_{uq}uq + M_{vr}vr + M_{|w|q}\sqrt{v^2+w^2}\,q \\ N_{ur}ur + N_{wr}wr + N_{vq}vq + N_{|v|r}\sqrt{v^2+w^2}\,r \end{bmatrix} \tag{9}$$

$$+ \begin{bmatrix} X_{uu}u|u| + X_{vv}v^2 + X_{ww}w^2 \\ Y_{uu}u^2 + Y_{uv}uv + Y_{vw}vw + Y_{v|v|}v\sqrt{v^2+w^2} \\ Z_{uu}u^2 + Z_{vv}v^2 + Z_{uw}u|w| + Z_{w|w|}w\sqrt{v^2+w^2} + Z_{ww}|w|\sqrt{v^2+w^2} \\ M_{uu}u^2 + M_{vv}v^2 + M_{uw}uw + M_{u|w|}u|w| + M_{ww}|w|\sqrt{v^2+w^2} + M_{w|w|}w\sqrt{v^2+w^2} \\ N_{uu}u^2 + N_{uv}uv + N_{vw}vw + N_{v|v|}v\sqrt{v^2+w^2} \end{bmatrix}.$$

The control inputs τ_R in (2) caused by rudders, propellers, and bow thrusters gives

$$\tau_R = \begin{bmatrix} X_{\text{prop}} \\ u|u|Y_{\delta_r}\delta_r + Y_{\text{prop}} \\ u|u|Z_{\delta_s}\delta_s + Z_{\text{prop}} \\ \left(u|u|M_{\delta_s} + u|q|M_{|q|\delta_s}\right)\delta_s + z_B B\sin\theta \\ \left(u|u|N_{\delta_r} + u|r|N_{|r|\delta_r}\right)\delta_r \end{bmatrix}. \tag{10}$$

The lumped disturbances τ_d in (2) can be shown as follows:

$$\tau_d = \left[\tau_{d1}, \tau_{d2}, \tau_{d3}, \tau_{d4}, \tau_{d_5}\right]^T. \tag{11}$$

According to the terms mentioned above, expanding the dynamic model in (1) yields

$$\left(m - \frac{1}{2}\rho L^3 X'_{\dot{u}}\right)\dot{u} = mvr - mwq + \frac{1}{2}\rho L^4\left[X'_{qq}q^2 + X'_{rr}r^2\right] + \frac{1}{2}\rho L^3\left[X'_{vr}vr + X'_{wq}wq\right] + \frac{1}{2}\rho L^2\left[X'_{uu}u|u| + X'_{vv}v^2 + X'_{ww}w^2\right] + X_{\text{prop}} + \tau_{d1}, \tag{12}$$

$$\left(m - \frac{1}{2}\rho L^3 Y'_{\dot{v}}\right)\dot{v} - \frac{1}{2}\rho L^4 Y'_{\dot{r}}\dot{r} = -mur + \frac{1}{2}\rho L^4\left[Y'_{qr}qr + Y'_{r|r|}r|r|\right] + \frac{1}{2}\rho L^3\left[Y'_{ur}ur + Y'_{vq}vq + Y'_{wr}wr + Y'_{v|r|}\frac{v}{|v|}\sqrt{v^2+w^2}\,|r|\right] + \frac{1}{2}\rho L^2 u|u|Y'_{\delta_r}\delta_r + \frac{1}{2}\rho L^2\left[Y'_{uu}u^2 + Y'_{uv}uv + Y'_{vw}vw + Y'_{v|v|}v\sqrt{v^2+w^2}\right] + Y_{prop} + \tau_{d2}, \tag{13}$$

$$\left(m - \frac{1}{2}\rho L^3 Z'_{\dot{w}}\right)\dot{w} - \frac{1}{2}\rho L^4 Z'_{\dot{q}}\dot{q} = muq + \frac{1}{2}\rho L^4\left[Z'_{rr}r^2 + Z'_{q|q|}q|q|\right] + \frac{1}{2}\rho L^2\left[Z'_{uu}u^2 + Z'_{vv}Z'_{vv}v^2 + Z'_{uw}uw + Z'_{u|w|}u|w| + Z'_{w|w|}w\sqrt{v^2+w^2} + Z'_{ww}|w|\sqrt{v^2+w^2}\right] + \frac{1}{2}\rho L^3\left[Z'_{uq}uq + Z'_{vr}vr + Z'_{w|q|}\frac{w}{|w|}\sqrt{v^2+w^2}\,|q|\right] + \frac{1}{2}\rho L^2 u|u|Z'_{\delta_s}\delta_s + Z_{\text{prop}} + \tau_{d3}, \tag{14}$$

$$\begin{aligned}\left(I_y-\frac{1}{2}\rho L^5M'_{\dot{q}}\right)\dot{q}-\frac{1}{2}\rho L^4M'_{\dot{w}}\dot{w}&=\frac{1}{2}\rho L^5\left[M'_{q|q|}q|q|+M'_{rr}r^2\right]\\&+\frac{1}{2}\rho L^4\left[M'_{uq}uq+M'_{vr}vr+M'_{|w|\dot{q}}\sqrt{v^2+w^2}\,q\right]\\&+\frac{1}{2}\rho L^3\left[M'_{uu}u^2+M'_{vv}v^2+M'_{uw}uw+M'_{u|w|}u|w|+M'_{ww}|w|\sqrt{v^2+w^2}\right.\\&\left.+M'_{w|w|}w\sqrt{v^2+w^2}\right]\\&+\left(\frac{1}{2}\rho L^3u|u|M'_{\delta_s}+\frac{1}{2}\rho L^4u|q|M'_{|q|\delta_s}\right)\delta_s+z_BB\sin\theta+\tau_{d4},\end{aligned}\tag{15}$$

$$\begin{aligned}\left(I_z-\frac{1}{2}\rho L^5N'_{\dot{r}}\right)\dot{r}-\frac{1}{2}\rho L^4N'_{\dot{v}}\dot{v}&=\frac{1}{2}\rho L^5\left[N'_{r|r|}r|r|+N'_{qr}qr\right]\\&+\frac{1}{2}\rho L^4\left[N'_{ur}ur+N'_{wr}wr+N'_{vq}vq+N'_{|v|r}\sqrt{v^2+w^2}\,r\right]\\&+\frac{1}{2}\rho L^3\left[N'_{uu}u^2+N'_{uv}uv+N'_{vw}vw+N'_{v|v|}v\sqrt{v^2+w^2}\right]\\&+\left(\frac{1}{2}\rho L^3u|u|N'_{\delta_r}+\frac{1}{2}\rho L^4u|r|N'_{|r|\delta_r}\right)\delta_r+\tau_{d5},\end{aligned}\tag{16}$$

where L is the length of the UUV. The mathematical models of a single UUV can be further shown in the compact form according to equations (1)–(16):

$$\dot{\xi}=\begin{bmatrix}I & 0\\ 0 & M_f\end{bmatrix}^{-1}\begin{bmatrix}f'_1(\xi)\\ f'_2(\xi)\end{bmatrix}+\begin{bmatrix}I & 0\\ 0 & M_f\end{bmatrix}^{-1}\begin{bmatrix}0\\ \tau_d\end{bmatrix}+\begin{bmatrix}I & 0\\ 0 & M_f\end{bmatrix}^{-1}\begin{bmatrix}0\\ g'(\xi)\end{bmatrix}\widehat{u},\tag{17}$$

where $\xi=[x,y,z,\theta,\psi,u,v,w,q,r]^T$,

$$M_f=\begin{bmatrix}m-\frac{1}{2}\rho L^3X'_{\dot{u}} & 0 & 0 & 0 & 0\\ 0 & m-\frac{1}{2}\rho L^3Y'_{\dot{v}} & 0 & 0 & -\frac{1}{2}\rho L^4Y'_{\dot{r}}\\ 0 & 0 & m-\frac{1}{2}\rho L^3Z'_{\dot{w}} & -\frac{1}{2}\rho L^4Z'_{\dot{q}} & 0\\ 0 & 0 & -\frac{1}{2}\rho L^4M'_{\dot{w}} & I_y-\frac{1}{2}\rho L^5M'_{\dot{q}} & 0\\ 0 & -\frac{1}{2}\rho L^4N'_{\dot{v}} & 0 & 0 & I_z-\frac{1}{2}\rho L^5N'_{\dot{r}}\end{bmatrix}.\tag{18}$$

$g'(\xi)$ relating to the term $\widehat{u} = [\tau_u, \tau_v, \tau_w, \tau_s, \tau_r]^T$:

$$g'(\xi) = \begin{bmatrix} 1 & 0 & 0 & 0 & 0 \\ 0 & 1 & 0 & 0 & \frac{1}{2}\rho L^2 u|u| Y'_{\delta_r} \\ 0 & 0 & 1 & \frac{1}{2}\rho L^2 u|u| Z'_{\delta_s} & 0 \\ 0 & 0 & 0 & \frac{1}{2}\rho L^3 u|u| M'_{\delta_s} + \frac{1}{2}\rho L^4 M'_{|q|\delta_s} u|q| & 0 \\ 0 & 0 & 0 & 0 & \frac{1}{2}\rho L^3 u|u| N'_{\delta_r} + \frac{1}{2}\rho L^4 u|r| N'_{|r|\delta_r} \end{bmatrix}, \tag{19}$$

$f_1'(\xi)$ comprising the left-hand-side of the kinematics model in (1), and $f_2'(\xi)$ consisting of the remaining terms in the left-hand-side of equations (12)–(16) .

Then (17) can be rewritten as

$$\dot{\xi} = f(\xi) + g(\xi)\widehat{u}, \tag{20}$$

where $g(\xi) = \begin{bmatrix} I & 0 \\ 0 & M_f \end{bmatrix}^{-1} \begin{bmatrix} 0 \\ g'(\xi) \end{bmatrix} \in R^{10}$, $f(\xi) = [f_1(\xi), f_2(\xi)]^T \in \mathbb{R}^{10}$. Obviously, we can see that $f_1(\xi) = f_1'(\xi), f_1'(\xi) \in \mathbb{R}^5$, $f_2(\xi)$ includes $\overline{f}(\xi) = M_f^{-1} f_2'(\xi)$, $\overline{f}(\xi) \in \mathbb{R}^5$ and $D = M_f^{-1}\tau_d, D \in \mathbb{R}^5$ so that

$$f_2(\xi) = \overline{f}(\xi) + D. \tag{21}$$

This paper mainly investigates the cooperative control method for the UUV based on the earth-fixed coordinate system, so the position (x, y, z), pitch angle θ, and yaw angle ψ are defined as the output $h(\xi)$:

$$h(\xi) = \begin{bmatrix} x & y & z & \theta & \psi \end{bmatrix}^T. \tag{22}$$

2.4. Feedback Linearization. Feedback linearization has been becoming an important technique to nonlinear control design since it can tackle some practical control problems. The idea of the technique is to transform the nonlinear model into the linear one, and then some linear control design method can be applied.

Considering the following multiple input multiple output (MIMO) nonlinear system

$$\begin{aligned} \dot{x} &= f(x) + g(x)u, \\ y &= h(x), \end{aligned} \tag{23}$$

where $x \in \mathbb{R}^m, u \in \mathbb{R}^p$, and $y \in \mathbb{R}^q$ are the state variables, the input, and output of the system, respectively. $f(x)$, $g(x)$, and $h(x)$ are system function with an appropriate dimension.

Definition 1 (see [44]) (MIMO System Relative Degrees). The MIMO nonlinear system (23), $p = q$, is said to have relative degrees $\rho_1, \rho_2, \ldots, \rho_p$, if

(1) $L_{g_j} L_f^k h_i(x) = 0$, $1 \le i \le p$, $1 \le j \le p$, $0 \le k < \rho_i - 1$, and for any i, $1 \le i \le p$, there exists at least one j, such that $L_{g_j} L_f^{\rho_i - 1} h_i(x) \ne 0$;

(2) The matrix $\Upsilon(x)$ is nonsingular,

$$\Upsilon(x) = \begin{bmatrix} L_{g_1} L_f^{\rho_1 - 1} h_1(x) & L_{g_2} L_f^{\rho_1 - 1} h_1(x) & \cdots & L_{g_p} L_f^{\rho_1 - 1} h_1(x) \\ L_{g_1} L_f^{\rho_2 - 1} h_2(x) & L_{g_2} L_f^{\rho_2 - 1} h_2(x) & \cdots & L_{g_p} L_f^{\rho_2 - 1} h_2(x) \\ \vdots & \vdots & \ddots & \vdots \\ L_{g_1} L_f^{\rho_p - 1} h_p(x) & \cdots & \cdots & L_{g_p} L_f^{\rho_p - 1} h_p(x) \end{bmatrix}. \tag{24}$$

Define the relative degrees of system (23) as $\rho = \rho_1 + \rho_2 + \cdots + \rho_p$.

Definition 1 can lead to a sufficient condition of feedback linearization for the MIMO system (23).

Lemma 1 (see [44]). *The nonlinear system (23) can be transformed into the linearization system if the following conditions can be satisfied:*

(1) The affine nonlinear system requires input and output numbers are the same, $p = q$

(2) The affine nonlinear system exists the relative degree $\rho_1, \rho_2, \ldots, \rho_p$

(3) The sum of relative degree ρ_i is the same as the dimension of the nonlinear system, $\rho = m$

Proof. The affine nonlinear system exists the relative degree $\rho_1, \rho_2, \ldots, \rho_p$, so a new set of state variables can be given

$$\begin{aligned}
\phi_1^i &= h_i(x),\\
\phi_2^i &= L_f h_i(x),\\
&\vdots\\
\phi_{\rho_i}^i &= L_f^{\rho_i - 1} h_i(x),\\
&\qquad 1 \le i \le p.
\end{aligned} \tag{25}$$

The first $\rho_i - 1$ state equations transform as

$$\dot{\phi}_k^i = \phi_{k+1}^i, \quad k = 1, \ldots, (\rho_i - 1), \tag{26}$$

and the last state equation is

$$\dot{\phi}_{\rho_i}^i = \varsigma_i(\phi) + \sum_{j=1}^{p} \zeta_{ij}(\phi) u_j, \quad 1 \le i \le p, \tag{27}$$

where $\varsigma_i(\phi) = L_f^{\rho_i} h_i(x)$ and $\zeta_{ij}(\phi) = L_{g_j} L_f^{\rho_i - 1} h_i(x)$.

Then define new input v:

$$v = \Phi(\phi) + \Upsilon(\phi) u, \tag{28}$$

where $\Phi(\phi) = [\varsigma_1(\phi), \varsigma_2(\phi), \ldots, \varsigma_p(\phi)]^T$,

$$\Upsilon(\phi) = \begin{bmatrix} \zeta_{11}(\phi) & \cdots & \zeta_{1p}(\phi) \\ \vdots & \ddots & \vdots \\ \zeta_{p1}(\phi) & \cdots & \zeta_{pp}(\phi) \end{bmatrix}. \tag{29}$$

According to Definition 1, the matrix $\Upsilon(\phi)$ is nonsingular, so the feedback input of the system (23) can be shown as follows:

$$u = \Upsilon^{-1}(\phi)(v - \Phi(\phi)). \tag{30}$$

Consequently, after the state and the input of the system transformed, we can obtain the following linear equations:

$$\begin{aligned}
\dot{\phi}_1^i &= \phi_2^i,\\
&\vdots\\
\dot{\phi}_{\rho_i - 1}^i &= \phi_{\rho_i}^i,\\
\dot{\phi}_{\rho_i}^i &= v_i,\\
&\qquad 1 \le i \le p.
\end{aligned} \tag{31}$$

□

2.5. Feedback Linearization for the UUV Model. The nonlinear model for an UUV in 5 DOF and the feedback linearization technique are introduced above. In this subsection, the nonlinear UUV model is transformed into a double-integrator dynamic model by the feedback linearization technique.

The system (20) and the system output (22) can be written in the form

$$\begin{aligned}
\dot{\xi} &= f(\xi) + g(\xi)\widehat{u},\\
y &= h(\xi),
\end{aligned} \tag{32}$$

where $\xi = [x, y, z, \theta, \psi, u, v, w, q, r]^T$, $f(\xi) = [f_1(\xi), f_2(\xi), \ldots, f_{10}(\xi)]^T$, $g(\xi) = [g_1(\xi), \ldots, g_5(\xi)]$, $\widehat{u} = [\tau_u, \tau_v, \tau_w, \tau_s, \tau_r]^T$, and $h(\xi) = [h_1(\xi), \ldots, h_5(\xi)]^T$.

As mentioned above, the vector $f(\xi)$ is known as follows:

$$\begin{aligned}
f_1(\xi) &= u\cos\psi\cos\theta - v\sin\psi + w\cos\psi\sin\theta,\\
f_2(\xi) &= u\sin\psi\cos\theta + v\cos\psi + w\sin\psi\sin\theta,\\
f_3(\xi) &= -u\sin\theta + w\cos\theta,\\
f_4(\xi) &= q,\\
f_5(\xi) &= \frac{r}{\cos\theta},\\
f_6(\xi) &= \overline{f}_1(\xi) + D_1,\\
f_7(\xi) &= \overline{f}_2(\xi) + D_2,\\
f_8(\xi) &= \overline{f}_3(\xi) + D_3,\\
f_9(\xi) &= \overline{f}_4(\xi) + D_4,\\
f_{10}(\xi) &= \overline{f}_5(\xi) + D_5.
\end{aligned} \tag{33}$$

From terms 6 to 10 in (33), they are denoted by the symbol $f_6(\xi)$–$f_{10}(\xi)$, since they are less affected on the feedback linearization method.

The system output function is

$$\begin{aligned}
h_1(\xi) &= x,\\
h_2(\xi) &= y,\\
h_3(\xi) &= z,\\
h_4(\xi) &= \theta,\\
h_5(\xi) &= \psi.
\end{aligned} \tag{34}$$

According to (17), $g(\xi) = \begin{bmatrix} I & 0 \\ 0 & M_f \end{bmatrix}^{-1} \begin{bmatrix} 0 \\ g'(\xi) \end{bmatrix}$, the nonzero values $g(\xi) = [g_{ij}(\xi)]$, $1 \le i \le 10$, $1 \le j \le 5$ can be represented as follows:

In the first column of $g(\xi)$,

$$g_{61}(\xi) = \frac{1}{m - (1/2)\rho L^3 X'_{\dot{u}}}. \tag{35}$$

In the second column of $g(\xi)$,

$$g_{72}(\xi) = \frac{I_z - (1/2)\rho L^5 N_{\dot{r}}'}{\left(m - (1/2)\rho L^3 Y_{\dot{v}}'\right)\left(I_z - (1/2)\rho L^5 N_{\dot{r}}'\right) - \left((1/2)\rho L^4 Y_{\dot{r}}'\right)\left((1/2)\rho L^4 N_{\dot{v}}'\right)},$$
$$g_{10,2}(\xi) = \frac{(1/2)\rho L^4 N_{\dot{v}}'}{\left(m - (1/2)\rho L^3 Y_{\dot{v}}'\right)\left(I_z - (1/2)\rho L^5 N_{\dot{r}}'\right) - \left((1/2)\rho L^4 Y_{\dot{r}}'\right)\left((1/2)\rho L^4 N_{\dot{v}}'\right)}. \tag{36}$$

In the third column of $g(\xi)$,

$$g_{83}(\xi) = \frac{I_y - (1/2)\rho L^5 M_{\dot{q}}'}{\left(m - (1/2)\rho L^3 Z_{\dot{w}}'\right)\left(I_y - (1/2)\rho L^5 M_{\dot{q}}^{v}\right) - \left((1/2)\rho L^4 Z_{\dot{q}}'\right)\left((1/2)\rho L^4 M_{\dot{w}}'\right)},$$
$$g_{93}(\xi) = \frac{(1/2)\rho L^4 M_{\dot{w}}'}{\left(m - (1/2)\rho L^3 Z_{\dot{w}}'\right)\left(I_y - (1/2)\rho L^5 M_{\dot{q}}'\right) - \left((1/2)\rho L^4 Z_{\dot{q}}'\right)\left((1/2)\rho L^4 M_{\dot{w}}'\right)}. \tag{37}$$

In the fourth column of $g(\xi)$,

$$g_{84}(\xi) = \frac{(1/2)\rho L^2 u|u| Z_{\delta_s}'\left(I_y - (1/2)\rho L^5 M_{\dot{q}}'\right) + \left((1/2)\rho L^3 u|u| M_{\delta_s}' + (1/2)\rho L^4 M_{|q|\delta_s}' u|q|\right)\left((1/2)\rho L^4 Z_{\dot{q}}'\right)}{\left(m - (1/2)\rho L^3 Z_{\dot{w}}'\right)\left(I_y - (1/2)\rho L^5 M'\right)_{\dot{q}} - \left((1/2)\rho L^4 Z_{\dot{q}}'\right)\left((1/2)\rho L^4 M_{\dot{w}}'\right)}$$
$$g_{94}(\xi) = \frac{\left((1/2)\rho L^3 u|u| M_{\delta_s}' + (1/2)\rho L^4 M_{|q|\delta_s}' u|q|\right)\left(m - (1/2)\rho L^3 Z_{\dot{w}}'\right) + \left((1/2)\rho L^2 u|u| Z_{\delta_s}'\right)\left((1/2)\rho L^4 M_{\dot{w}}'\right)}{\left(m - (1/2)\rho L^3 Z_{\dot{w}}'\right)\left(I_y - (1/2)\rho L^5 M_{\dot{q}}'\right) - \left((1/2)\rho L^4 Z_{\dot{q}}'\right)\left((1/2)\rho L^4 M_{\dot{w}}'\right)}. \tag{38}$$

In the fifth column of $g(\xi)$,

$$g_{75}(\xi) = \frac{(1/2)\rho L^2 u|u| Y_{\delta_r}'\left(I_z - (1/2)\rho L^5 N_{\dot{r}}'\right) + \left((1/2)\rho L^3 u|u| N_{\delta_r}' + (1/2)\rho L^4 u|r| N_{|r|\delta_r}'\right)\left((1/2)\rho L^4 N_{\dot{v}}'\right)}{\left(m - (1/2)\rho L^3 Y_{\dot{v}}'\right)\left(I_z - (1/2)\rho L^5 N_{\dot{r}}'\right) - \left((1/2)\rho L^4 Y_{\dot{r}}'\right)\left((1/2)\rho L^4 N_{\dot{v}}'\right)},$$
$$g_{10,5}(\xi) = \frac{\left((1/2)\rho L^3 u|u| N_{\delta_r}' + (1/2)\rho L^4 u|r| N_{|r|\delta_r}'\right)\left(m - (1/2)\rho L^3 Y_{\dot{v}}'\right) + \left((1/2)\rho L^2 u|u| Y_{\delta_r}'\right)\left((1/2)\rho L^4 N_{\dot{v}}'\right)}{\left(m - (1/2)\rho L^3 Y_{\dot{v}}'\right)\left(I_z - (1/2)\rho L^5 N_{\dot{r}}'\right) - \left((1/2)\rho L^4 Y_{\dot{r}}'\right)\left((1/2)\rho L^4 N_{\dot{v}}'\right)}. \tag{39}$$

According to the matrix $g(\xi)$, we can conclude that for any i and j, $1 \le i \le 5$, $1 \le j \le 5$, so that

$$L_{g_i} h_j(\xi) = 0. \tag{40}$$

Then the Lie derivative of $h(\xi)$ with respect to $f(\xi)$ is shown as follows:

$$\begin{aligned}
L_f h_1(\xi) &= u\cos\psi\cos\theta - v\sin\psi + w\cos\psi\sin\theta,\\
L_f h_2(\xi) &= u\sin\psi\cos\theta + v\cos\psi + w\sin\psi\sin\theta,\\
L_f h_3(\xi) &= -u\sin\theta + w\cos\theta,\\
L_f h_4(\xi) &= q,\\
L_f h_5(\xi) &= \frac{r}{\cos\theta}.
\end{aligned} \tag{41}$$

From (33)–(41), it follows that $\Upsilon(\xi)$ can be calculated as

$$\Upsilon(\xi)=\begin{bmatrix} g_{6,1}\cos\psi\cos\theta & -g_{7,2}\sin\psi & g_{8,3}\cos\psi\sin\theta & g_{8,4}\cos\psi\sin\theta & -g_{7,5}\sin\psi \\ g_{6,1}\sin\psi\cos\theta & g_{7,2}\cos\psi & g_{8,3}\sin\psi\sin\theta & g_{8,4}\sin\psi\sin\theta & g_{7,5}\cos\psi \\ -g_{6,1}\sin\theta & 0 & g_{8,3}\cos\theta & g_{8,4}\cos\theta & 0 \\ 0 & 0 & g_{9,3} & g_{9,4} & 0 \\ 0 & \dfrac{g_{10,2}}{\cos\theta} & 0 & 0 & \dfrac{g_{10,5}}{\cos\theta} \end{bmatrix}. \tag{42}$$

It can see that $\Upsilon(\xi)$ is nonsingular according to $g_{ij}(\xi)$ when $u\neq 0$, so the nonlinear model of UUV exists the relative degree:

$$\begin{aligned} \rho_1&=2,\\ \rho_2&=2,\\ \rho_3&=2,\\ \rho_4&=2,\\ \rho_5&=2. \end{aligned} \tag{43}$$

It can be seen that $\rho_1+\rho_2+\rho_3+\rho_4+\rho_5=10=m$, so the technique of the state feedback linearization is applicable to the nonlinear model of the UUV according to Lemma 1, then the two vectors are defined as follows:

$$\begin{aligned} x&=\left[\,h_1(\xi)\;\; h_2(\xi)\;\; h_3(\xi)\;\; h_4(\xi)\;\; h_5(\xi)\,\right]^T\in\mathbb{R}^5,\\ \nu&=\left[\,L_fh_1(\xi)\;\; L_fh_2(\xi)\;\; L_fh_3(\xi)\;\; L_fh_4(\xi)\;\; L_fh_5(\xi)\,\right]^T\in\mathbb{R}^5. \end{aligned} \tag{44}$$

Define the following control input of the UUV which would be applied in the linearization system:

$$\widetilde{u}=\Phi(\xi)+\Upsilon(\xi)\widehat{u}, \tag{45}$$

where $\Phi(\xi)=\left[\,L_f^2h_1(\xi)\;\; L_f^2h_2(\xi)\;\; L_f^2h_3(\xi)\;\; L_f^2h_4(\xi)\;\; L_f^2h_5(\xi)\,\right]^T$,

$$\begin{aligned} L_f^2h_1(\xi)&=(-u\cos\psi\sin\theta+w\cos\psi\cos\theta)f_4(\xi)+(-u\sin\psi\cos\theta-v\cos\psi)f_5(\xi)\\ &\quad -w\sin\psi\sin\theta f_5(\xi)+\cos\psi\cos\theta f_6(\xi)-\sin\psi f_7(\xi)+\cos\psi\sin\theta f_8(\xi)\\ &=(-u\cos\psi\sin\theta+w\cos\psi\cos\theta)f_4(\xi)-(u\sin\psi\cos\theta+v\cos\psi)f_5(\xi)\\ &\quad -w\sin\psi\sin\theta f_5(\xi)+\cos\psi\cos\theta\left(\overline{f}_6(\xi)+D_1\right)-\sin\psi\left(\overline{f}_7(\xi)+D_2\right)+\cos\psi\sin\theta\left(\overline{f}_8(\xi)+D_3\right)\\ &=(-u\cos\psi\sin\theta+w\cos\psi\cos\theta)f_4(\xi)-(u\sin\psi\cos\theta+v\cos\psi)f_5(\xi)-w\sin\psi\sin\theta f_5(\xi)\\ &\quad +\cos\psi\cos\theta\overline{f}_6(\xi)-\sin\psi\overline{f}_7(\xi)+\cos\psi\sin\theta\overline{f}_8(\xi)+\overline{D}_1,\\ L_f^2h_2(\xi)&=(-u\sin\psi\sin\theta+w\sin\psi\cos\theta)f_4(\xi)+(u\cos\psi\cos\theta-v\sin\psi)f_5(\xi)\\ &\quad +w\cos\psi\sin\theta f_5(\xi)+\sin\psi\cos\theta f_6(\xi)+\cos\psi f_7(\xi)+\sin\psi\sin\theta f_8(\xi)\\ &=(-u\sin\psi\sin\theta+w\sin\psi\cos\theta)f_4(\xi)+(u\cos\psi\cos\theta-v\sin\psi)f_5(\xi)\\ &\quad +w\cos\psi\sin\theta f_5(\xi)+\sin\psi\cos\theta\overline{f}_6(\xi)+\cos\psi\overline{f}_7(\xi)+\sin\psi\sin\theta\overline{f}_8(\xi)+\overline{D}_2,\\ L_f^2h_3(\xi)&=(-u\cos\theta-w\sin\theta)f_4(\xi)-\sin\theta f_6(\xi)+\cos\theta f_8(\xi)\\ &=(-u\cos\theta-w\sin\theta)f_4(\xi)-\sin\theta\overline{f}_6(\xi)+\cos\theta\overline{f}_8(\xi)+\overline{D}_3,\\ L_f^2h_4(\xi)&=f_9(\xi)=\overline{f}_9(\xi)+\overline{D}_4,\\ L_f^2h_5(\xi)&=\frac{r\sin\theta}{\cos^2\theta}f_4(\xi)+\frac{f_{10}(\xi)}{\cos\theta}=\frac{r\sin\theta}{\cos^2\theta}f_4(\xi)+\frac{\overline{f}_{10}(\xi)}{\cos\theta}+\overline{D}_5. \end{aligned} \tag{46}$$

It is observed $\Phi(\xi) = \overline{\Phi}(\xi) + d$, where $d = [\overline{D}_1, \overline{D}_2, \overline{D}_3, \overline{D}_4, \overline{D}_5]^T$ are the disturbances. Since the input of the UUV can be shown as $\widetilde{u} = \Phi(\xi) + \Upsilon(\xi)\widehat{u}$, we can further obtain:

$$\widetilde{u} = \overline{\Phi}(\xi) + d + \Upsilon(\xi)\widehat{u} = u + d. \tag{47}$$

Consequently, the standard second-order integral form of the mathematical model of the UUV can be denoted as follows:

$$\begin{aligned} \dot{x} &= v, \\ \dot{v} &= u + d, \end{aligned} \tag{48}$$

where $x \in \mathbb{R}^5$, $v \in \mathbb{R}^5$, and $d \in \mathbb{R}^5$ present the position information, the velocity information, and the disturbances of the UUV, respectively.

To summarize, the second-order linear model of the UUV (48) can be accomplished by the state feedback linearization method. The coupled system can be transformed into a decoupled system, which contributes to the design of the cooperative controller quickly and conveniently. However, as the physical meanings of the partial state and the input of the UUV model can vary in the feedback linearization method, the new output of the controller by state feedback linearization method would not directly be applied in the original UUV model. In order to solve the problem, we apply the method of linearization transformation. After using the transformation, the output of the cooperative controller can be applied to the original UUV model.

2.6. The Extended State Observer. The extended state observer (ESO) method to reject the uncertainties in the system was proposed by Han [45]. By using a tracking-differentiator with the observer form, the ESO for a class of uncertain systems of the form $x^{(n)}(t) = f(x, \dot{x}, \ldots, x^{(n-1)}, t) + \omega(t)$ was given in the paper. It was shown, by choosing a proper nonlinear function and related parameters of the observer, the ESO can track the states of a class of uncertain plants.

3. Problem Formulation

Consider the multi-UUVs system with unmeasurable disturbances, including N followers and a leader.

The i-th UUV dynamics of the followers is shown as follows:

$$\begin{aligned} \dot{x}_i(t) &= v_i(t), \\ \dot{v}_i(t) &= u_i(t) + d_i(t), \\ y_i(t) &= x_i(t), \\ i &= 1, 2, \ldots, N, \end{aligned} \tag{49}$$

where $x_i(t) \in \mathbb{R}^5$, $v_i(t) \in \mathbb{R}^5$, and $d_i(t) \in \mathbb{R}^5$ are the position information state, the velocity information state, and unmeasurable disturbances, respectively. The dynamics (49) can be expressed in the following compact form:

$$\begin{aligned} \dot{\xi}_i(t) &= A\xi_i(t) + B(u_i(t) + d_i(t)), \\ y_i(t) &= C\xi_i(t), \\ i &= 1, \ldots, N, \end{aligned} \tag{50}$$

where $\xi_i(t) = \begin{bmatrix} x_i^T(t) & v_i^T(t) \end{bmatrix}^T \in \mathbb{R}^{10}$, $A = \begin{bmatrix} 0_5 & I_5 \\ 0_5 & 0_5 \end{bmatrix}$, $B = \begin{bmatrix} 0_5 & I_5 \end{bmatrix}^T$, and $C = \begin{bmatrix} I_5 & 0_5 \end{bmatrix}$.

Note that the i-th UUV can only exchange the position information state with its local neighbours in the paper.

The dynamics of the leader UUV is

$$\begin{aligned} \dot{x}_0(t) &= v_0(t), \\ y_0(t) &= x_0(t), \end{aligned} \tag{51}$$

where $x_0 \in \mathbb{R}^5$ and $v_0 \in \mathbb{R}^5$ are the position state and velocity state of the leader. Write the compact form obtained in (21) to the case of the dynamics as follows:

$$\begin{aligned} \dot{\xi}_0(t) &= A\xi_0(t), \\ y_0(t) &= C\xi_0(t), \end{aligned} \tag{52}$$

where $\xi_0 = \begin{bmatrix} x_0^T(t) & v_0^T(t) \end{bmatrix}^T \in \mathbb{R}^{10}$, $A = \begin{bmatrix} 0_5 & I_5 \\ 0_5 & 0_5 \end{bmatrix}$, and $C = \begin{bmatrix} I_5 & 0_5 \end{bmatrix}$.

Note that the leader is independent of the following UUVs and sends the information state to the part of the followers.

To design the consensus algorithm and analyze the stability for the system (50) and (52), the following definition, lemma, and assumption are necessary

Definition 2. The multi-UUVs system (50) and (52) is said to reach consensus asymptotically if there exists control input u_i for any initial state $\xi_i(t_0)$, $i = 1, \ldots, N$, $\lim_{t \longrightarrow \infty} \|\xi_i(t) - \xi_0(t)\| = 0$, $i = 1, \ldots, N$.

Assumption 1. The unmeasurable disturbances $d_i(t)$ denote the lumped disturbance and satisfy the following conditions: (1) $d_i(t)$ and $\dot{d}_i(t)$ are bounded; (2) $\lim_{t \longrightarrow \infty} d_i(t) = N_c$, where N_c is the unknown constant vector; (3) $\lim_{t \longrightarrow \infty} \dot{d}_i(t) = 0$.

Remark 1. The lumped disturbances which have a constant value in the steady state consist of unknown uncertainties and external disturbances. For more details about the lumped disturbances, please refer to [46]. In the relative work [29], we can find out the method on addressing the lumped disturbances in a multi-AUVs system, in which the disturbance observer estimated the lumped disturbances to compensate for the disturbances for multi-AUVs.

Lemma 2 (see [47]). *The following differential system $\dot{x}(t) = Ax(t) + Bu(t)$ is asymptotically stable if A is a Hurwitz matrix, $u(t)$ is bound, and $\lim_{t \longrightarrow \infty} u(t) = 0$.*

3.1. Leader-Following Multi-UUVs Consensus with Unmeasurable Disturbances under the Fixed Topology. In the subsection, the leader-following multi-UUVs consensus is discussed using the algorithm proposed in the paper, in

which each UUV suffered from unmeasurable disturbances in the fixed communication network. The controller design is heavily inspired by the work [41]; however, the detailed analysis and derivation for the stability in the proof of the Theorem 1 are from a different perspective in the subsection, which is beneficial to have preliminary knowledge about the next subsection, namely, the case with switching topologies.

In the subsection, the DESO which uses the relative local neighbour UUVs position information state to estimate the velocity information and disturbances is firstly shown. Then the leader-followers consensus algorithm which uses the estimation information from local neighbors DESO is exhibited. Finally, it is presented that the consensus control described in the subsection can be accomplished by Lyapunov function method Riccati inequality.

According to the control method of the standard ESO [45] adding an extended variable $d_i(t) \in \mathbb{R}^5$ to the system (49), the extended system for each following UUV can be presented as follows:

$$\begin{aligned} \dot{x}_i(t) &= v_i(t), \\ \dot{v}_i(t) &= u_i(t) + d_i(t), \\ \dot{d}_i(t) &= s_i(t), \\ y_i(t) &= x_i(t), \\ & \qquad i = 1, 2, \ldots, N, \end{aligned} \tag{53}$$

where $s_i(t) \in \mathbb{R}^5$.

The compact extended system for (53) can be written as

$$\begin{aligned} \dot{\overline{\xi}}_i(t) &= \overline{A}\overline{\xi}_i(t) + \overline{B}u_i(t) + Hs_i(t), \\ y_i(t) &= \overline{C}\overline{\xi}_i(t), \end{aligned} \tag{54}$$

where $\overline{\xi}_i(t) = \begin{bmatrix} x_i^T(t) & v_i^T(t) & d_i^T(t) \end{bmatrix}^T$, $\overline{A} = \begin{bmatrix} 0_5 & I_5 & 0_5 \\ 0_5 & 0_5 & I_5 \\ 0_5 & 0_5 & 0_5 \end{bmatrix}$, $\overline{B} = \begin{bmatrix} 0_5 & I_5 & 0_5 \end{bmatrix}^T$, $\overline{C} = \begin{bmatrix} I_5 & 0_5 & 0_5 \end{bmatrix}$, and $H = \begin{bmatrix} 0_5 & 0_5 & I_5 \end{bmatrix}^T$.

For the extended system (54), the DESO based on the relative position information state is designed as follows:

$$\begin{aligned} \dot{\hat{\overline{\xi}}}_i(t) &= \overline{A}\hat{\overline{\xi}}_i(t) + \overline{B}u_i(t) + \varphi_i(t), \\ \hat{y}_i(t) &= \overline{C}\hat{\overline{\xi}}_i(t), \end{aligned} \tag{55}$$

where $\hat{\overline{\xi}}_i(t) = \begin{bmatrix} \hat{x}_i^T(t) & \hat{v}_i^T(t) & \hat{d}_i^T(t) \end{bmatrix}^T$, $\hat{x}_i(t)$, and $\hat{v}_i(t)$ are the position and velocity state estimation for each UUV, respectively, $\hat{d}_i(t)$ means the disturbances estimation and

$$\varphi_i(t) = E\left(\sum_{j=1}^{N} a_{ij}\left[\tilde{y}_i(t) - \tilde{y}_j(t) \right] + q_i \tilde{y}_i(t) \right), \tag{56}$$

with a_{ij} and q_i are shown in the subsection 2.2 Graph theory, the observer gain $E \in \mathbb{R}^{15\times 5}$ is discussed later, and $\tilde{y}_i(t) = \hat{y}_i(t) - y_i(t)$.

The consensus algorithm in the case of fixed topology is shown as

$$u_i(t) = K \sum_{j\in N_i} a_{ij}\left(\hat{\xi}_i(t) - \hat{\xi}_j(t) \right) + q_i K\left(\hat{\xi}_i(t) - \xi_0(t) \right) - \hat{d}_i(t), \tag{57}$$

where $K \in \mathbb{R}^{5\times 10}$ is feedback control gain to be explained later. Note that the algorithm (57) is determined by the state estimation information instead of the information themselves and adopts the active disturbance rejection control scheme which would remove the disturbances effectively.

To analyze the stability of the closed-loop multi-UUVs system in the fixed topology, the following assumption is proposed as follows:

Assumption 2. The graph G among following UUVs is undirected, and the graph $\overline{G}$ is connected, in which the leader UUV has a directed path to the any following UUVs.

The states and disturbances estimation error are defined as follows:

$$\begin{aligned} \varepsilon_\xi(t) &= \hat{\xi}(t) - \xi(t), \\ \varepsilon_d(t) &= \hat{d}(t) - d(t), \end{aligned} \tag{58}$$

where $\xi(t) = \begin{bmatrix} \xi_1^T(t) & \ldots & \xi_N^T(t) \end{bmatrix}^T$, $\hat{\xi}(t) = \begin{bmatrix} \hat{\xi}_1^T(t) & \ldots & \hat{\xi}_N^T(t) \end{bmatrix}^T$, $d(t) = \begin{bmatrix} d_1^T(t) & \ldots & d_N^T(t) \end{bmatrix}^T$ and $\hat{d}(t) = \begin{bmatrix} \hat{d}_1^T(t) & \ldots & \hat{d}_N^T(t) \end{bmatrix}^T$.

Combining (54), (55), and (58), the estimation error equation can be given as follows:

$$\dot{\varepsilon}(t) = \left((I_N \otimes \overline{A}) + (F \otimes E\overline{C}) \right)\varepsilon(t) - (I_N \otimes H)S(t), \tag{59}$$

where $\varepsilon(t) = \begin{bmatrix} \varepsilon_\xi^T(t) & \varepsilon_d^T(t) \end{bmatrix}^T$ and $S(t) = \begin{bmatrix} s_1^T(t) & \ldots & s_N^T(t) \end{bmatrix}^T$.

Then the tracking error for the leader UUV and the following UUVs is defined as follows:

$$e(t) = \xi(t) - \xi_0(t). \tag{60}$$

Combining (50), (52), and (57), the tracking error equation is given as follows:

$$\dot{e}(t) = \left((I_N \otimes A) + (F \otimes BK) \right)e(t) + \begin{bmatrix} (F \otimes BK) & -(I_N \otimes B) \end{bmatrix}\varepsilon(t). \tag{61}$$

Lemma 3 (see [42]). *The matrix F is symmetric positive defined under Assumption 2.*

Finally, we show the main result of the leader-following consensus algorithm under unmeasurable disturbances with the fixed topology.

Theorem 1. *Suppose that Assumption 1 and Assumption 2 are satisfied. For the system (49) and (51) under control law (57), the leader-following multi-UUVs consensus is guaranteed if the symmetrical positive-define matrix P_1 and P_2 are, respectively, the solutions to Riccati inequality (62) and (63), $E = -\varsigma P_1^{-1}\overline{C}^T$ and $K = -\varsigma B^T P_2$ with $\varsigma \geq (1/\lambda_{\min}(F))$ being a positive constant.*

$$\overline{A}^T P_1 + P_1 \overline{A} - 2\overline{C}^T \overline{C} < 0, \tag{62}$$

$$A^T P_2 + P_2 A - 2P_2 B B^T P_2 < 0. \tag{63}$$

Proof. As the structure matrix F is symmetric positive definite under Assumption 2 and Lemma 3, there exists orthogonal matrix $U \in \mathbb{R}^{N\times N}$ such that

$$U^T F U = \operatorname{diag}(\lambda_1, \lambda_2, \ldots, \lambda_N) = \Lambda, \tag{64}$$

where $\lambda_i > 0$, $i = 1, \ldots, N$ is the eigenvalue of the matrix F.

Setting $\overline{\varepsilon}(t) = (U^T \otimes I_{15})\varepsilon(t)$, $\overline{e}(t) = (U^T \otimes I_{10})e(t)$, and $\overline{S}(t) = (U^T \otimes I_5)S(t)$, (59) and (61) can be written as follows:

$$\dot{\overline{\varepsilon}}(t) = \left[(I_N \otimes \overline{A}) + (\Lambda \otimes E\overline{C})\right]\overline{\varepsilon}(t) - (I_N \otimes H)\overline{S}(t), \tag{65}$$

$$\dot{\overline{e}}(t) = \left((I_N \otimes A) + (\Lambda \otimes BK)\right)\overline{e}(t) + \left[\begin{array}{cc} \Lambda \otimes BK & -I_N \otimes B \end{array}\right]\overline{\varepsilon}(t). \tag{66}$$

It thus follows that the leader-following multi-UUVs consensus can be reached asymptotically under designing the feedback control gain K and observer gain E such that the error systems (65) and (66) can asymptotically converge to zero, as $t \longrightarrow \infty$ by taking two steps. □

Step 1. According to (65), there exists a symmetrical positive-define matrix P_1 and we have

$$\begin{aligned} &\left((I_N \otimes \overline{A}) + (\Lambda \otimes E\overline{C})\right)^T (I_N \otimes P_1) + (I_N \otimes P_1)\left((I_N \otimes \overline{A}) + (\Lambda \otimes E\overline{C})\right) \\ &= I_N \otimes \overline{A}^T P_1 + I_N \otimes P_1 \overline{A} + \Lambda \otimes \overline{C}^T E^T P_1 + \Lambda \otimes P_1 E\overline{C}. \end{aligned} \tag{67}$$

Defining $E = -\varsigma P_1^{-1} \overline{C}^T$ with $\varsigma \geq (1/\lambda_{\min}(\Lambda))$ and substituting E into (67) yields

$$\begin{aligned} &\sum_{i=1}^{N} \overline{A}^T P_1 + P_1 \overline{A}_1 + \lambda_i(\Lambda)\left(\overline{C}^T E^T P_1 + P_1 E\overline{C}\right) \\ &\quad \leq \sum_{i=1}^{N} \overline{A}^T P_1 + P_1 \overline{A}_1 - 2\overline{C}^T \overline{C}. \end{aligned} \tag{68}$$

It follows from (62) that

$$\begin{aligned} &\left((I_N \otimes \overline{A}) + (\Lambda \otimes E\overline{C})\right)^T (I_N \otimes P_1) + (I_N \otimes P_1)\left((I_N \otimes \overline{A}) \right. \\ &\left. + (\Lambda \otimes E\overline{C})\right) < 0, \end{aligned} \tag{69}$$

which means the matrix $(I_N \otimes \overline{A}) + (\Lambda \otimes E\overline{C})$ is a Hurwitz matrix based on the Lyapunov stability theorem. Under Assumption 1, $\lim_{t\longrightarrow\infty} \overline{S}(t) = 0$ and $(I_N \otimes \overline{A}) + (\Lambda \otimes E\overline{C})$ being a Hurwitz matrix, it is concluded from Lemma 2 that estimation error system (65) satisfy $\lim_{t\longrightarrow\infty} \overline{\varepsilon}(t) = 0$, which implies $\lim_{t\longrightarrow\infty} \varepsilon(t) = 0$. It can be observed the DESO can estimate unmeasurable disturbances.

Step 2. Take the method like step 1 to show the multi-UUVs consensus tracking error can asymptotically converge to zero, as $t \longrightarrow \infty$.

According to (66), there exists a symmetrical positive-define matrix P_2 and we have

$$\begin{aligned} &\left((I_N \otimes A) + (\Lambda \otimes BK)\right)^T (I_N \otimes P_2) + (I_N \otimes P_2)\left((I_N \otimes A) \right. \\ &\left. + (\Lambda \otimes BK)\right) \\ &= I_N \otimes A^T P_2 + I_N \otimes P_2 A + \Lambda \otimes K^T B^T P_2 + \Lambda \otimes P_2 BK. \end{aligned} \tag{70}$$

Defining $K = -\varsigma B^T P_2$ with $\varsigma \geq (1/\lambda_{\min}(\Lambda))$ and substituting K into (70) yields

$$\begin{aligned} &\sum_{i=1}^{N} A^T P_2 + P_2 A + \lambda_i(\Lambda)\left(K^T B^T P_2 + P_2 BK\right) \\ &\quad \leq \sum_{i=1}^{N} A^T P_2 + P_2 A - 2P_2 B B^T P_2. \end{aligned} \tag{71}$$

It follows from (63) that

$$\begin{aligned} &\left((I_N \otimes A) + (\Lambda \otimes BK)\right)^T (I_N \otimes P_2) + (I_N \otimes P_2)\left((I_N \otimes A) \right. \\ &\left. + (\Lambda \otimes BK)\right) < 0, \end{aligned} \tag{72}$$

which means $((I_N \otimes A) + (\Lambda \otimes BK))$ is a Hurwitz matrix according to the Lyapunov stability theorem. It concludes from Lemma 2 that the tracking error system (66) satisfies $\lim_{t\longrightarrow\infty} \overline{e}(t) = 0$ under the above result $\lim_{t\longrightarrow\infty} \overline{\varepsilon}(t) = 0$ and $((I_N \otimes A) + (\Lambda \otimes BK))$ being a Hurwitz matrix. This implies that the state of the following UUVs can follow the state of the leader UUV.

The above analysis shows that $\lim_{t\longrightarrow\infty} \varepsilon(t) = 0$ and $\lim_{t\longrightarrow\infty} e(t) = 0$ under Assumption 1 and Lemma 2, which means estimation error and the tracking error can converge to zero as $t \longrightarrow \infty$ and the multi-UUVs system can achieve consensus under the consensus algorithm (57). The proof is completed.

3.2. Leader-Following Multi-UUVs Consensus with Unmeasurable Disturbances under the Switching Topology. This section extends the result in the previous section to the case multi-UUVs system under switching topologies with disturbances. From the previous section and this section, the difference and comparison between the case of fixed and switching topologies can be shown clearly.

For the extended system (54), the DESO in the condition of changing topology based on the relative position information state is designed as follows:

$$\begin{aligned} \dot{\widehat{\overline{\xi}}}_i(t) &= \overline{A}\widehat{\overline{\xi}}_i(t) + \overline{B}u_i(t) + \varphi_i(t), \\ \widehat{y}_i(t) &= \overline{C}\widehat{\overline{\xi}}_i(t), \end{aligned} \tag{73}$$

where $\varphi_i(t) = E(\sum_{j\in N_i(t)} a_{ij}(t)[\widetilde{y}_i(t) - \widetilde{y}_j(t)] + q_i(t)\widetilde{y}_i(t))$.

The consensus algorithm under changing topology is designed as follows:

$$\begin{aligned} u_i(t) = K &\sum_{j\in N_i(t)} a_{ij}(t)\left(\widehat{\xi}_i(t) - \widehat{\xi}_j(t)\right) + q_i(t)K\left(\widehat{\xi}_i(t) - \xi_0(t)\right) \\ &- \widehat{d}_i(t). \end{aligned} \tag{74}$$

Note that the consensus algorithm in the section is different from the case in the last section. In the section, each UUV needs information from its neighbours and the communication topology is changing dynamically because of unreliable communication link underwater. $N_i(t)$, $a_{ij}(t)$, and $q_i(t)$ represent different communication topologies among UUVs over time.

Similar to the last section, the estimation error equation and the tracking error equation can be written as follows:

$$\dot{\varepsilon}(t) = \left[(I_N \otimes \overline{A}) + \left(F_{\rho(t)} \otimes E\overline{C}\right)\right]\varepsilon(t) - (I_N \otimes H)S(t), \tag{75}$$

$$\begin{aligned}\dot{e}(t) = {} & \left[(I_N \otimes A) + \left(F_{\rho(t)} \otimes BK\right)\right]e(t) \\ & + \left[\left(F_{\rho(t)} \otimes BK\right) - (I_N \otimes B)\right]\varepsilon(t),\end{aligned} \tag{76}$$

where $F_{\rho(t)} = L_{\rho(t)} + Q_{\rho(t)}$.

In the section, the graph shows that the communication topology may be dynamically changing over time. Use $\left\{\overline{G}_{\rho(t)}\colon \rho(t) \longrightarrow \ell\right\}$ to denote a graph set of all possible graphs for the leader UUV and following UUVs, where ℓ is the index set for all graphs and $\rho\colon [0, \infty) \longrightarrow \ell$ is changing signal at time t. $\left\{G_{\rho(t)}\colon \rho(t) \longrightarrow \ell\right\}$ shows a graph set of all possible graphs among the following UUVs.

Definition 3 (see [48]). The union of a collection of graphs is a graph whose node and edge sets are the unions of the node and edge sets of the graphs in the collection. It is said that the union of the collection of the graphs is jointly connected when the union graph is connected.

For the time-varying communication topology, as treated in [49], consider an infinite sequence of a contiguous, nonempty, and bounded time interval $[t_k, t_{k+1})$, $k = 0, 1, \ldots$, starting with $t_0 = 0$ with $t_{k+1} - t_k \le T$, $T > 0$. Suppose each interval $[t_k, t_{k+1})$ can be divided into z_k nonoverlapping subintervals:

$$\left[t_k^0, t_k^1\right), \left[t_k^2, t_k^3\right), \ldots, \left[t_k^{z_k-1}, t_k^{z_k}\right), \quad t_k = t_k^0,\ t_{k+1} = t_k^{z_k}, \tag{77}$$

with $t_k^{i+1} - t_k^i > \kappa$, $0 \le i \le z_k - 1$ where $\kappa > 0$ meaning the dwell time of the topology in the subinterval. The communication topology described as $\overline{G}(\rho(t_k^i))$ in each subinterval is fixed. The graph $\overline{G}(\rho(t_k^i)), i = 0, \ldots, z_k - 1$ can be disconnected in the subinterval $\left[t_k^i\ \ t_k^{i+1}\right)$, $0 \le i \le z_k - 1$, but the union graph $\overline{G}(\rho(t_k^i))$, $i = 0, \ldots, z_k - 1$ is jointly connected across the interval $[t_k, t_{k+1})$, $k = 0, 1, \ldots$ in the paper, so we present the following assumption:

Assumption 3. The union graph is jointly connected cross the time interval $[t_k, t_{k+1})$, $k = 0, 1, \ldots$.

Before analyzing the stability of the multi-UUVs system under the switching topology in presence of the unmeasurable disturbances, it is necessary to investigate the eigenvalue of the structure matrix $F_f = L_f + Q_f$, $f \in \ell$ associated with the graph $\overline{G}_f$. For the eigenvalue of the matrix F_f, we firstly investigate the eigenvalue of the matrix F_f^i related to the subpart graphs $\overline{G}_f^i$ of the graph $\overline{G}_f$ and further present the eigenvalue of the structure matrix F_f associated with graph $\overline{G}_f$.

The graph G_f consists of n_f subpart graphs G_f^i, $1 \le i \le n_f$ which is $G_f^i = (V(G_f^i), E(G_f^i))$, $1 \le i \le n_f$. The Laplacian of the subpart graph G_f^i is $L_f^i \in \mathbb{R}^{s_f^i \times s_f^i}$, $s_f^i = |V(G_f^i)|$ and the matrix Q_f^i of the subpart graph is shown as $Q_f^i = \mathrm{diag}(q_f^{i_1}, q_f^{i_2}, \ldots, q_f^{i_{s_f^i}})$. The structure matrix associated with the subpart graph $\overline{G}_f^i$ can be shown as $F_f^i = L_f^i + Q_f^i$. Therefore, the structure matrix F_f associated with a graph $\overline{G}_f$ can be represented as $F_f = \mathrm{diag}(F_f^1, \ldots, F_f^{n_f})$.

Next, we proceed to obtain the eigenvalue of the structure matrix F_f associated with the graph $\overline{G}_f$. For each matrix F_f^i associated with the subpart graphs $\overline{G}_f^i$, the matrix F_f^i has $s_f^i = |V(G_f^i)|$ nonnegative eigenvalues where $V(G_f^i) = \left\{\nu_1^i\ \ \nu_2^i\ \ \cdots\ \ \nu_{s_f^i}^i\right\}$ with $\left\{\nu_1^i\ \ \nu_2^i\ \ \cdots\ \ \nu_{s_f^i}^i\right\} \subset \{1\ \ 2\ \ \ldots\ \ N\}$ and $\nu_1^i < \nu_2^i < \cdots < \nu_{s_f^i}^i$. The nonnegative eigenvalues of the matrix F_f^i are denoted as $\left\{\lambda_1^i\ \ \lambda_2^i\ \ \cdots\ \ \lambda_{s_f^i}^i\right\}$ and $\lambda_1^i \le \lambda_2^i \le \cdots \le \lambda_{s_f^i}^i$. Match the nodes sequence $\left\{\nu_1^i, \nu_2^i, \ldots, \nu_{s_f^i}^i\right\}$ of the subpart graphs $\overline{G}_f^i$ with the nonnegative eigenvalues sequence $\left\{\lambda_1^i, \lambda_2^i, \ldots, \lambda_{s_f^i}^i\right\}$ of the matrix F_f^i, denoting as $\nu_j^i \longleftrightarrow \lambda_j^i$, $j = 1, 2, \ldots, s_f^i$.

Then we have the nonnegative eigenvalues of the matrix F_f by lumping together with the nonnegative eigenvalues of each matrix F_f^i, $1 \le i \le n_f$ associated with the subpart graphs $\overline{G}_f^i$, $1 \le i \le n_f$. The method investigating the eigenvalue of the structure matrix F_f is shown by the following example.

Example 1. Consider one leader UUV is labeled as 0 and four following UUVs are labeled as 1 to 4. The graph G_f consists of two subpart graphs G_f^1 and G_f^2 seen in Figure 2. The structure matrices F_f^1 and F_f^2 can be represented as follows:

$$\begin{aligned} F_f^1 &= L_f^1 + Q_f^1 = \begin{bmatrix} 2 & -1 & 0 \\ -1 & 2 & -1 \\ 0 & -1 & 1 \end{bmatrix}, \\ F_f^2 &= 0. \end{aligned} \tag{78}$$

The eigenvalues sequence of the matrix F_f^1 are $\{0.1981\ \ 1.5550\ \ 3.2470\}$ and the sequence of the nodes of the subpart graphs G_f^1 is $\{1\ \ 3\ \ 4\}$. Matching the nodes sequence of the subpart graphs $\overline{G}_f^1$ with the nonnegative eigenvalue sequence of the matrix F_f^1 are $1 \longleftrightarrow 0.1981$, $3 \longleftrightarrow 1.5550$, $4 \longleftrightarrow 3.2470$. The eigenvalues sequence of the matrix F_f^2 is $\{0\}$ and the nodes sequence of the subpart graphs G_f^2 is $\{2\}$. Match the eigenvalue and node as $2 \longleftrightarrow 0$. Then the eigenvalues of the structure matrix F_f are $\{0.1981\ \ 0\ \ 1.5550\ \ 3.2470\}$.

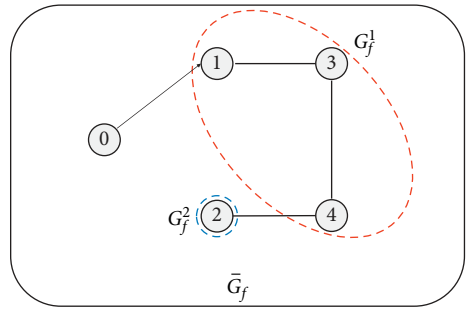

Figure 2: The graph $\overline{G}_f$ and its subpart graphs $\overline{G}_f^i$.

We define,

$$N(f) = \{j \mid j = 1, \ldots, N, \quad \text{the node corresponding to nonzero eigenvalue of structure maxtix}\}. \tag{79}$$

According to the definition above, we have $N(f) = \{1\ \ 3\ \ 4\}$ in example 1.

For each graph $f \in \ell$, $\lambda_{\min}(F_f)$ means the minimum eigenvalue of the structure matrix F_f described in Notation, and we further define $\gamma_{\min} = \min\{\lambda_{\min}(F_f), f \in \ell\}$ in this section.

We now show the main result of this section.

Theorem 2. *Suppose that Assumption 1 is satisfied and the switching graphs $\overline{G}_{\rho(t)}$ associated with changing communication topology satisfies Assumption 3. For systems (49) and (51) under control law (74), the leader-following multi-UUVs consensus is guaranteed if the symmetrical positive-define matrix P_1 and P_2 are, respectively, the solutions to Riccati inequality (80) and (81), $E = -\Gamma P_1^{-1}\overline{C}^T$ and $K = -\Gamma B^T P_2$ with $\Gamma \geq (1/\gamma_{\min})$ being a positive constant.*

$$\overline{A}^T P_1 + P_1 \overline{A} - 2\overline{C}^T \overline{C} < 0, \tag{80}$$

$$A^T P_2 + P_2 A - 2P_2 B B^T P_2 < 0. \tag{81}$$

Proof. It takes two steps to illustrate that error systems (75) and (76) can asymptotically converge to zero, as $t \longrightarrow \infty$. □

Step 1. The first step is to show that the estimation error can converge to zero, as $t \longrightarrow \infty$. We firstly investigate the case where the graph $\overline{G}_{\rho(t)}$, $\rho(t) = f$, $t = [\, t_k^i \ \ t_k^{i+1}\,)$, $i = 0, \ldots, z_k - 1$ is not changing, which implies the structure matrix F_f is symmetric.

As the structure matrix F_f is symmetric positive definite under Assumption 2 and Lemma 3, there exists orthogonal matrix $U \in \mathbb{R}^{N\times N}$ such that

$$U^T F_f U = \operatorname{diag}(\lambda_1, \lambda_2, \ldots, \lambda_N) = \Lambda_f, \tag{82}$$

where $\lambda_i > 0, i = 1, \ldots, N$ is the eigenvalue of the matrix F_f.

Setting $\overline{\varepsilon}(t) = (U^T \otimes I_{15})\varepsilon(t)$, $\overline{e}(t) = (U^T \otimes I_{10})e(t)$, and $\overline{S}(t) = (U^T \otimes I_5)S(t)$, (75) and (76) can be written as follows:

$$\dot{\overline{\varepsilon}}(t) = \left[(I_N \otimes \overline{A}) + \left(\Lambda_f \otimes E\overline{C}\right)\right]\varepsilon(t) - (I_N \otimes H)\overline{S}(t), \tag{83}$$

and

$$\begin{aligned}\dot{\overline{e}}(t) = &\left[(I_N \otimes A) + \left(\Lambda_f \otimes BK\right)\right]\overline{e}(t)\\ &+ \left[\left(\Lambda_f \otimes BK\right) \ -(I_N \otimes B)\right]\overline{\varepsilon}(t).\end{aligned} \tag{84}$$

According to (83), there exists a symmetrical positive-define matrix P_1. Define the Lyapunov candidate function $V(t) = \overline{\varepsilon}^T(t)(I_N \otimes P_1)\overline{\varepsilon}(t)$ which is continuously differentiable except the switching instant, and taking derivative of the Lyapunov candidate function with respect to time along the trajectory of estimation error dynamics,

$$\begin{aligned}\dot{V}(t) &= \dot{\overline{\varepsilon}}^T(I_N \otimes P_1)\overline{\varepsilon} + \overline{\varepsilon}^T(I_N \otimes P_1)\dot{\overline{\varepsilon}}\\ &= \overline{\varepsilon}(t)^T\Big(\left((I_N \otimes \overline{A}) + \left(\Lambda_f \otimes E\overline{C}\right)\right)^T(I_N \otimes P_1)\\ &\quad + (I_N \otimes P_1)\left((I_3 \otimes \overline{A}) + \left(\Lambda_f \otimes E\overline{C}\right)\right)\Big)\overline{\varepsilon}(t)\\ &= \sum_{i\in N(f)} \overline{\varepsilon}_i^T(t)\Big(\overline{A}^T P_1 + P_1\overline{A} + \lambda_i\left(\Lambda_f\right)\\ &\quad \cdot \left(\overline{C}^T E^T P_1 + P_1 E\overline{C}\right)\Big)\overline{\varepsilon}_i(t).\end{aligned} \tag{85}$$

Defining $E = -\Gamma P_1^{-1}\overline{C}^T$ with $\Gamma \geq (1/\gamma_{\min})$ and substituting E into (85), then it follows from (80) that $\dot{V}(t) \leq 0$ which means $\lim_{t\longrightarrow\infty} V(t)$ exists.

Considering the infinite sequence of $V(t)$, $t \in [\, t_{k+1} \ \ t_k\,)$, $k = 0, 1, \ldots$, according to Cauchy's convergence criteria, for any $\beta > 0$, there exists the positive integer N_β, and for any k with $k > N_\beta$, $|V(t_{k+1}) - V(t_k)| < \beta$, $k = 0, 1, \ldots$. We can rewrite the inequality as follows:

$$\left|\int_{t_k}^{t_{k+1}} \dot{V}(t)\mathrm{d}t\right| < \beta. \tag{86}$$

Equation (86) can be written as the following form of sum of the integrals:

$$\left|\int_{t_k^0}^{t_k^1}\dot{V}(t)\mathrm{d}t\right|+\cdots+\left|\int_{t_k^{z_k-1}}^{t_k^{z_k}}\dot{V}(t)\mathrm{d}t\right|<\beta. \tag{87}$$

According to the result $\dot{V}(t)\le 0$, let $\dot{V}(t)\le -a\sum_{i\in N(\rho(t_k^i))}\overline{\varepsilon}_i^T(t)\overline{\varepsilon}_i(t)$ with $\alpha>0$. Each integral $|\int_{t_k^i}^{t_k^{i+1}}\dot{V}(t)\mathrm{d}t|$ in (87) can be shown as follows:

$$\begin{aligned}\left|\int_{t_k^i}^{t_k^{i+1}}\dot{V}(t)\mathrm{d}t\right|&=\int_{t_k^i}^{t_k^{i+1}}-\dot{V}(t)\mathrm{d}t\ge a\int_{t_k^i}^{t_k^{i+1}}\sum_{i\in N\left(\rho\left(t_k^i\right)\right)}\overline{\varepsilon}_i^T(t)\overline{\varepsilon}_i(t)\mathrm{d}t\\&\ge a\int_{t_k^i}^{t_k^i+\kappa}\sum_{i\in N\left(\rho\left(t_k^i\right)\right)}\overline{\varepsilon}_i^T(t)\overline{\varepsilon}_i(t)\mathrm{d}t.\end{aligned} \tag{88}$$

Note $a\int_{t_k^i}^{t_k^i+\kappa}\sum_{i\in N(\rho(t_k^i))}\overline{\varepsilon}_i^T(t)\overline{\varepsilon}_i(t)\mathrm{d}t<\beta$, $i=0,1,\ldots,z_k-1$. For any $k>N_\beta$, we can have

$$\lim_{t\longrightarrow\infty}\int_t^{t+\kappa}\sum_{i\in N\left(\rho\left(t_k^i\right)\right)}\overline{\varepsilon}_i^T(\tau)\overline{\varepsilon}_i(\tau)\mathrm{d}\tau=0,\quad i=0,1,\ldots,z_k-1, \tag{89}$$

thus

$$\begin{aligned}\lim_{t\longrightarrow\infty}\int_t^{t+\kappa}\Bigg(&\sum_{i\in N\left(\rho\left(t_k^0\right)\right)}\overline{\varepsilon}_i^T(\tau)\overline{\varepsilon}_i(\tau)+\cdots+\\&\sum_{i\in N\left(\rho\left(t_k^{z_k-1}\right)\right)}\overline{\varepsilon}_i^T(\tau)\overline{\varepsilon}_i(\tau)\Bigg)\mathrm{d}\tau=0,\end{aligned} \tag{90}$$

which implies

$$\lim_{t\longrightarrow\infty}\int_t^{t+\kappa}\left(\sum_{i=1}^N\mu_i\overline{\varepsilon}_i^T(\tau)\overline{\varepsilon}_i(\tau)\right)\mathrm{d}\tau=0, \tag{91}$$

where μ_i, $i=1,\ldots,N$ is a positive integer.

Note that $\overline{\varepsilon}(t)$ is bounded according to $\dot{V}(t)\le 0$, so $\sum_{i=1}^N\overline{\varepsilon}_i^T(\tau)\overline{\varepsilon}_i(\tau)$ is uniformly continuous. Using Barbalat's lemma gives $\lim_{t\longrightarrow\infty}\sum_{i=1}^N\overline{\varepsilon}_i^T(t)\overline{\varepsilon}_i(t)=\lim_{t\longrightarrow\infty}\sum_{i=1}^N\varepsilon_i^T(t)\varepsilon_i(t)=0$, which implies $\lim_{t\longrightarrow\infty}\varepsilon_i(t)=0$, $i=1,\ldots,N$. It can be concluded that the DESO can effectively estimate the unmeasurable disturbances under the switching topology for multi-UUVs.

Step 2. The next step is to present that the position state and velocity state of the following UUVs can track that of the leader UUV with unmeasurable disturbances under switching topology. The method in the subsection is similar to the method in Step 1. We firstly discuss the graph $\overline{G}_{\rho(t)}$, $\rho(t)=f$, $t=\left[t_k^i\ t_k^{i+1}\right)$, $i=0,\ldots,z_k-1$ is not changing, which implies the structure matrix F_f is symmetric. According to (84), there exists the symmetrical positive-define matrix P_2. Consider the Lyapunov candidate function $V(t)=\overline{e}^T(t)(I_N\otimes P_2)\overline{e}(t)$ which is continuously differentiable except the switching instant. Under the previous result $\lim_{t\longrightarrow\infty}\varepsilon(t)=0$ in step 1, taking derivative of the Lyapunov candidate function with respect to time along the tracking error dynamics,

$$\begin{aligned}\dot{V}(t)=\sum_{i\in N(f)}\overline{e}^T(t)\Big(&A^TP_2+I_N\otimes P_2A+\Lambda_f\Big(K^TB^TP_2\\&+P_2BK\Big)\Big)\overline{e}(t).\end{aligned} \tag{92}$$

Defining $K=-\Gamma B^TP_2$ with $\Gamma\ge(1/\gamma_{\min})$ and substituting K into (91), then it follows from (81) that $\dot{V}(t)\le 0$ which means $\lim_{t\longrightarrow\infty}V(t)$ exists.

Considering an infinite sequence of $V(t)$, $t\in\left[t_{k+1}\ t_k\right)$, $k=0,1,\ldots,$ according to Cauchy's convergence criteria, for any $\eta>0$, there exists the positive integer N_η, and for any k with $k>N_\eta$, $|V(t_{k+1})-V(t_k)|<\eta$, $k=0,1,\ldots$ which is equivalent to

$$\left|\int_{t_k}^{t_{k+1}}\dot{V}(t)\mathrm{d}t\right|=\left|\int_{t_k^0}^{t_k^1}\dot{V}(t)\mathrm{d}t\right|+\cdots+\left|\int_{t_k^{z_k-1}}^{t_k^{z_k}}\dot{V}(t)\mathrm{d}t\right|<\eta. \tag{93}$$

Let $\dot{V}(t)\le -\sigma\sum_{i\in N(\rho(t_k^i))}\overline{e}_i^T(t)\overline{e}_i(t)$ with $\sigma>0$, then each integral in (93) can be shown as follows:

$$\begin{aligned}\left|\int_{t_k^i}^{t_k^{i+1}}\dot{V}(t)\mathrm{d}t\right|&=\int_{t_k^i}^{t_k^{i+1}}-\dot{V}(t)\mathrm{d}t\ge\sigma\int_{t_k^i}^{t_k^{i+1}}\sum_{i\in N\left(\rho\left(t_k^i\right)\right)}\overline{e}_i^T(t)\overline{e}_i(t)\mathrm{d}t\\&\ge a\int_{t_k^i}^{t_k^i+\kappa}\sum_{i\in N\left(\rho\left(t_k^i\right)\right)}\overline{e}_i^T(t)\overline{e}_i(t)\mathrm{d}t.\end{aligned} \tag{94}$$

For any $k>N_\eta$, we have

$$\lim_{t\longrightarrow\infty}\int_t^{t+\kappa}\sum_{i\in N\left(\rho\left(t_k^i\right)\right)}\overline{e}_i^T(\tau)\overline{e}_i(\tau)\mathrm{d}\tau=0,\quad i=0,1,\ldots,z_k-1, \tag{95}$$

then

$$\begin{aligned}\lim_{t\longrightarrow\infty}\int_t^{t+\kappa}\Bigg(&\sum_{i\in N\left(\rho\left(t_k^0\right)\right)}\overline{e}_i^T(\tau)\overline{e}_i(\tau)+\cdots+\\&\sum_{i\in N\left(\rho\left(t_k^{z_k-1}\right)\right)}\overline{e}_i^T(\tau)\overline{e}_i(\tau)\Bigg)\mathrm{d}\tau=0,\end{aligned} \tag{96}$$

which implies

$$\lim_{t\longrightarrow\infty}\int_t^{t+\kappa}\left(\sum_{i=1}^N\upsilon_i\overline{e}_i^T(\tau)\overline{e}_i(\tau)\right)\mathrm{d}\tau=0, \tag{97}$$

where υ_i, $i=1,\ldots,N$ is a positive integer.

Note that $e(t)$ is bounded according to $\dot{V}(t)\le 0$; therefore, $\sum_{i=1}^N\overline{e}_i^T(\tau)\overline{e}_i(\tau)$ is uniformly continuous. $\lim_{t\longrightarrow\infty}\sum_{i=1}^N\overline{e}_i^T(t)\overline{e}_i(t)=\lim_{t\longrightarrow\infty}\sum_{i=1}^Ne_i^T(t)e_i(t)=0$ holds by using Barbalat's lemma, which implies $\lim_{t\longrightarrow\infty}e_i(t)=0$, $i=1,\ldots,N$. It can be concluded that the multi-UUVs system (50) and (52) reach consensus under the consensus algorithm (74).

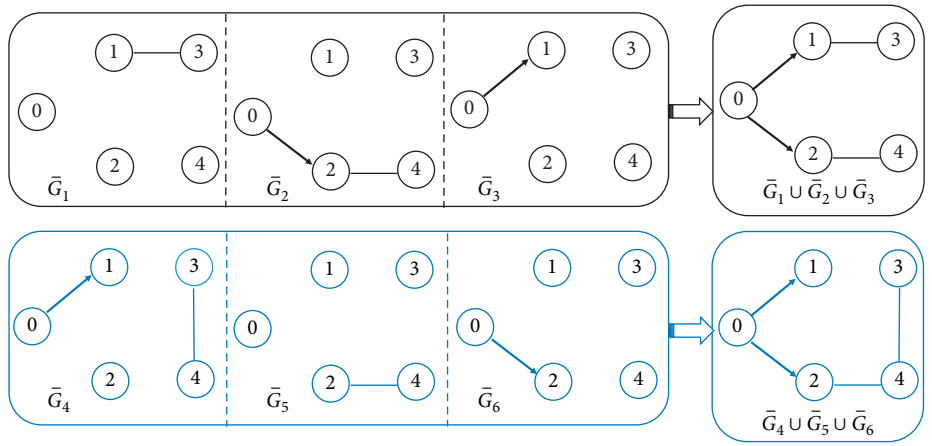

Figure 3: The communication topologies between UUV leader and UUV followers.

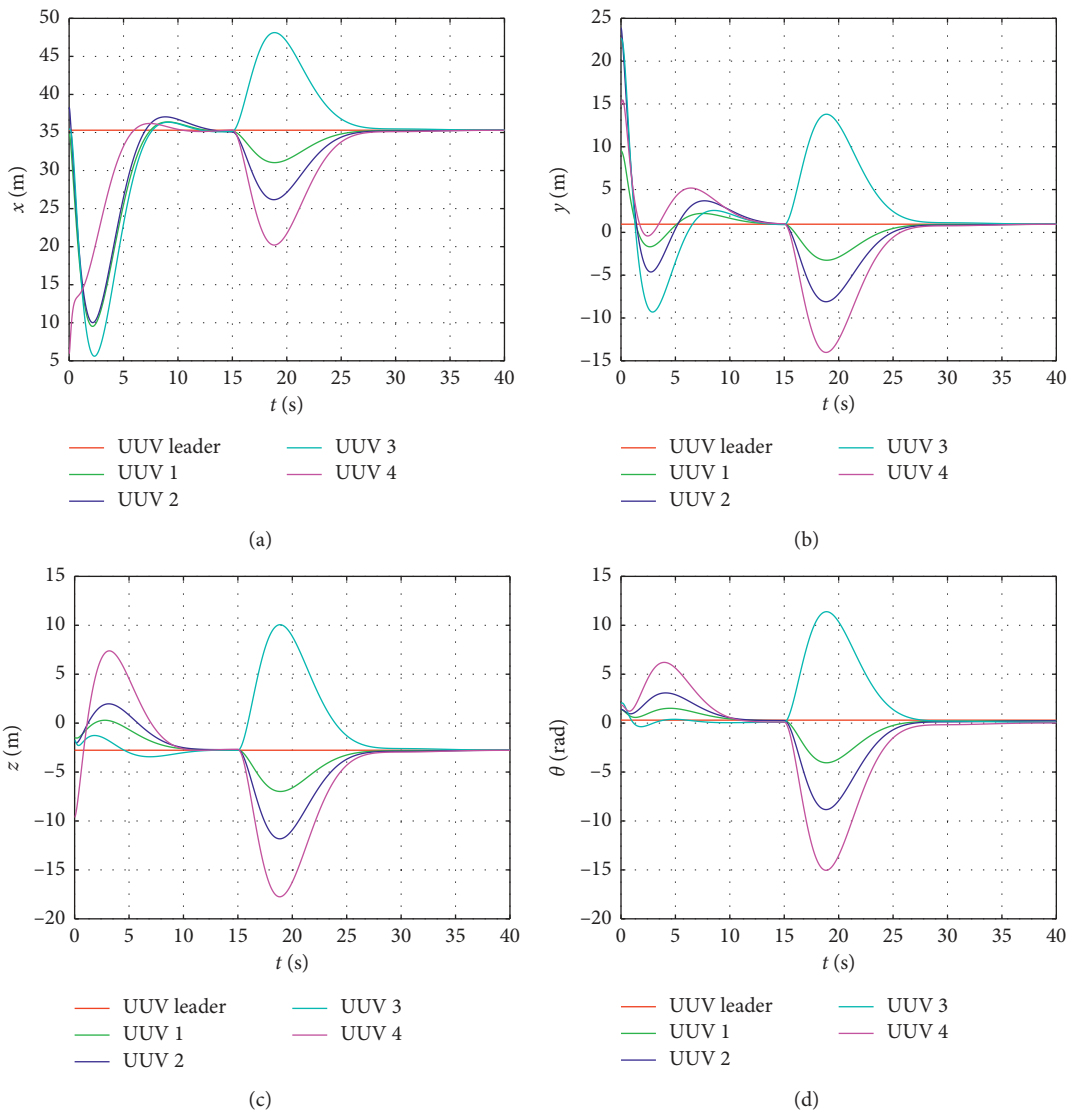

Figure 4: Continued.

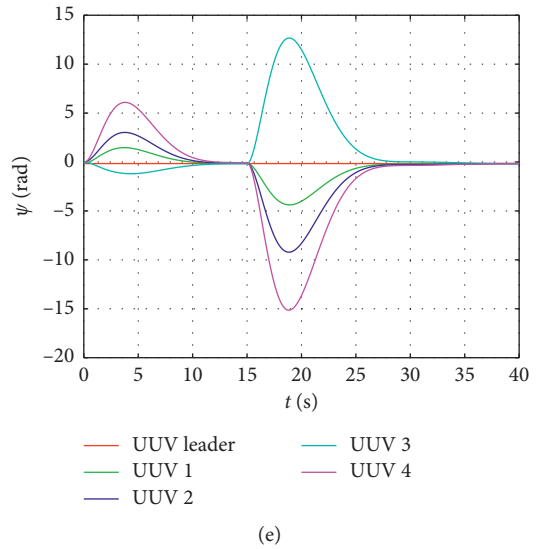

(e)

Figure 4: Position and attitude states of leader-following multi-UUVs with algorithm (74).

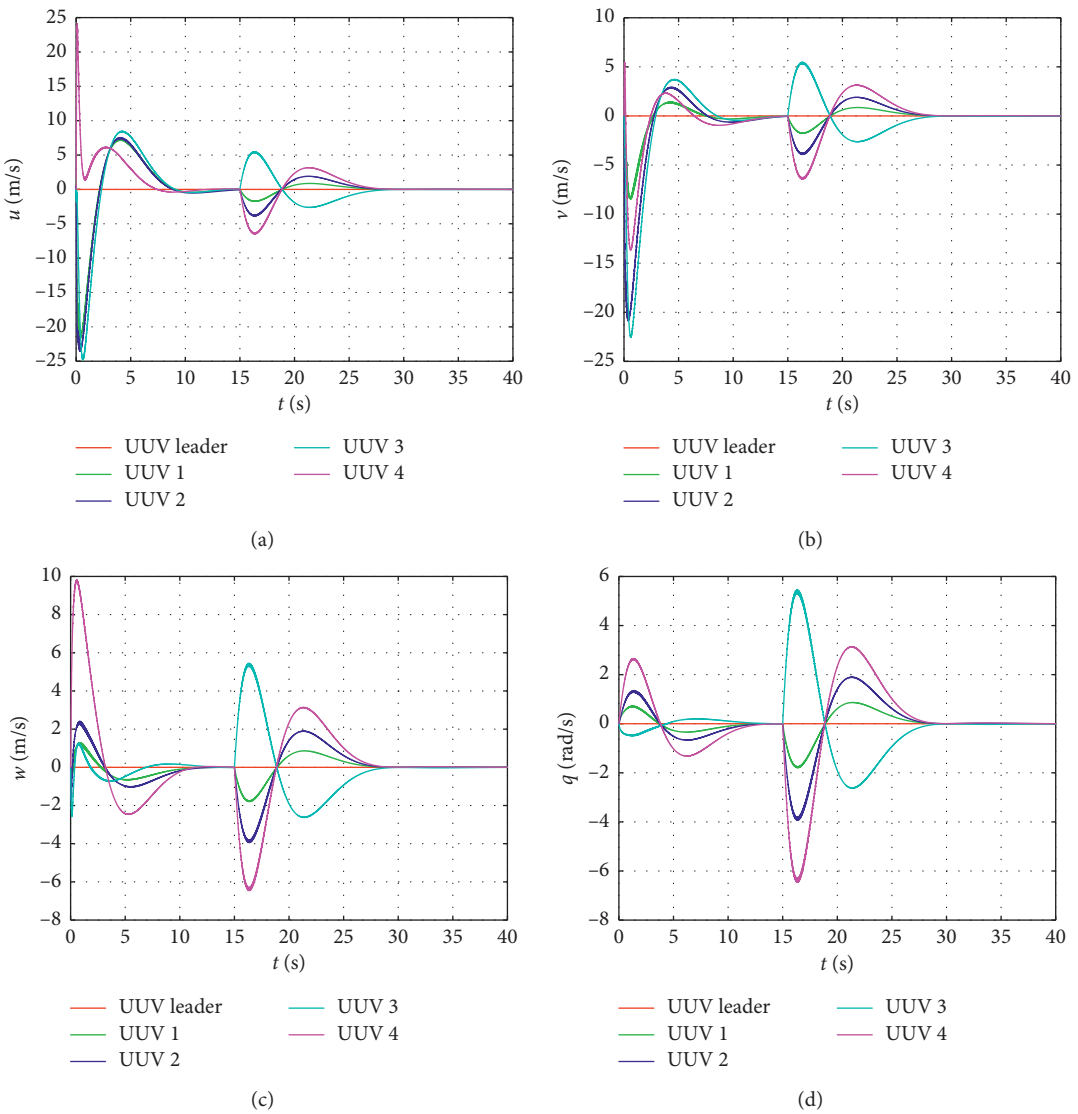

Figure 5: Continued.

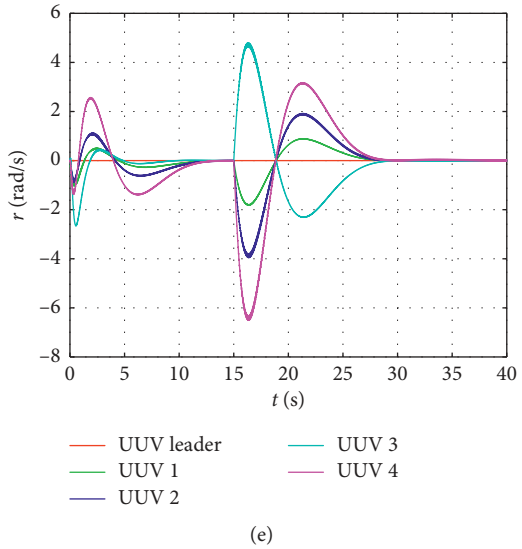

(e)

Figure 5: Velocity states of leader-following multi-UUVs with algorithm (74).

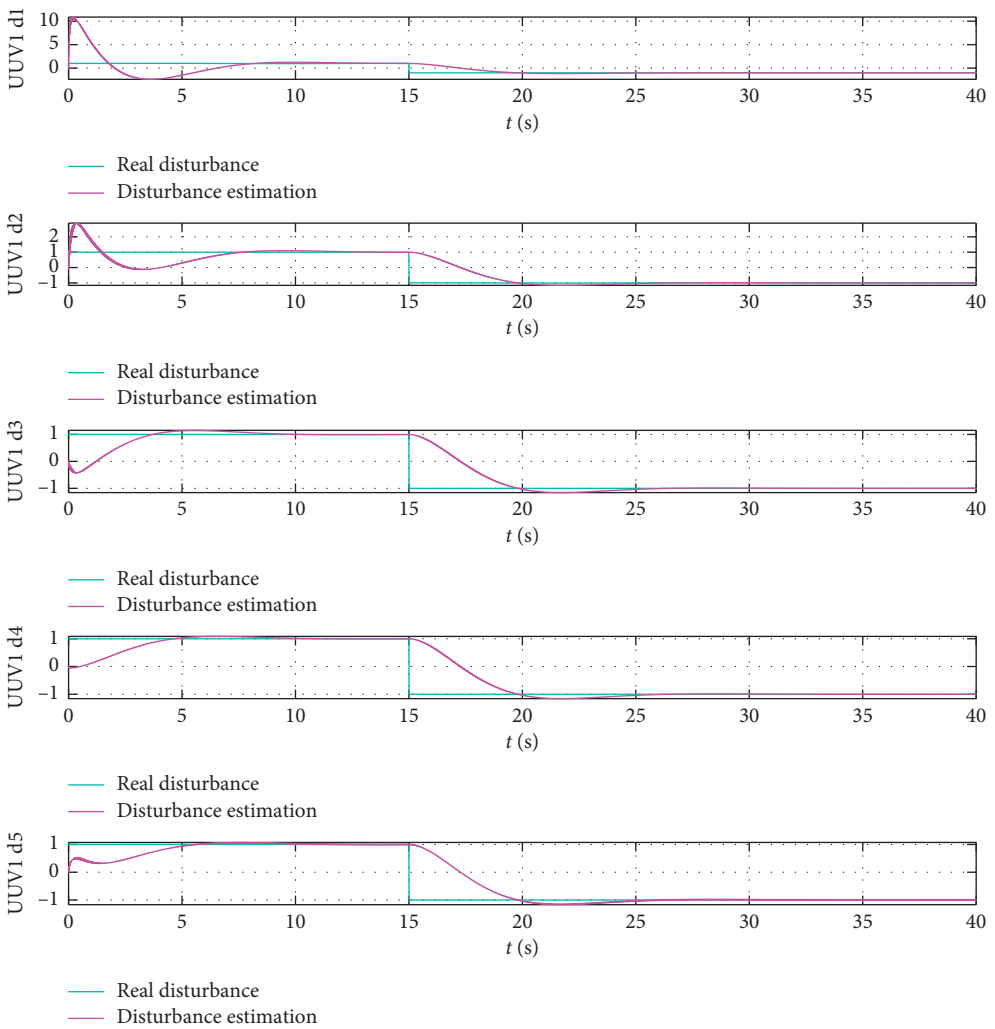

Figure 6: Comparison of real disturbance d_1 and disturbance estimation $\widehat{d}_1$.

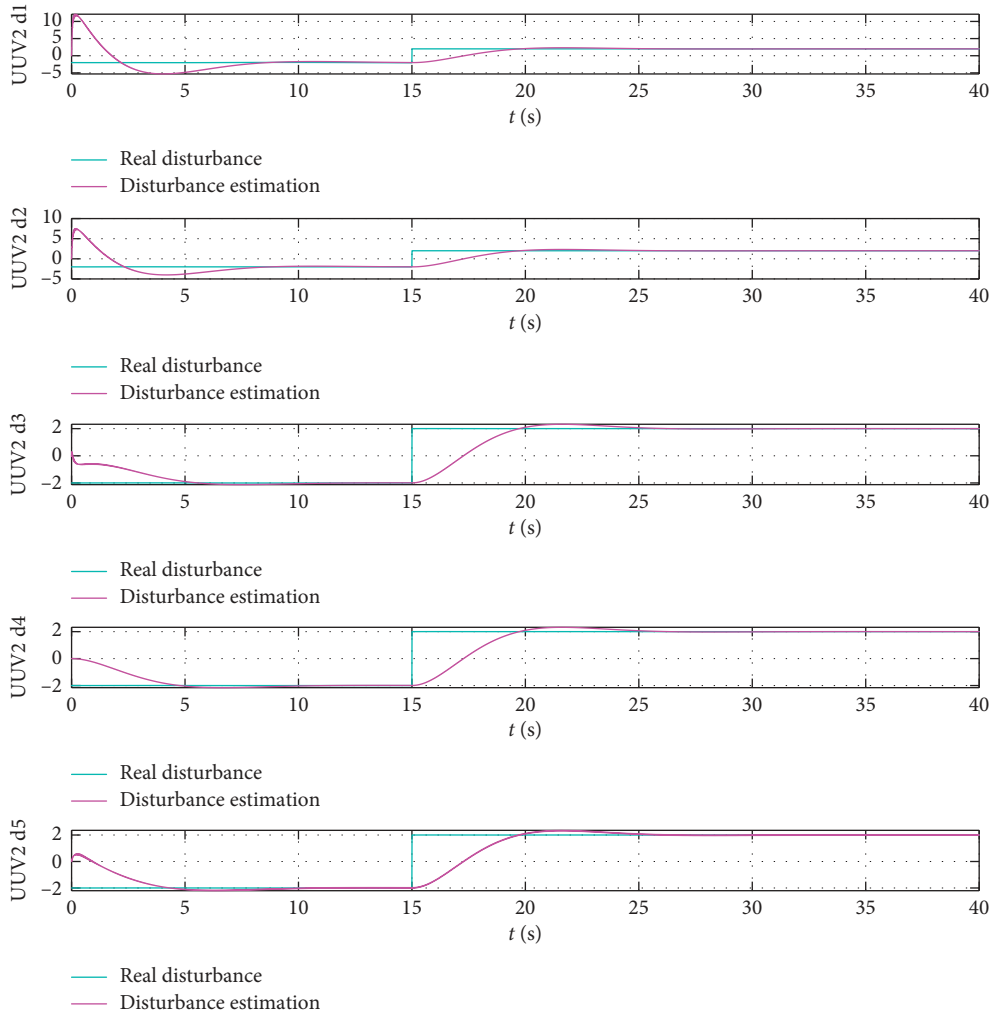

Figure 7: Comparison of real disturbance d_2 and disturbance estimation $\widehat{d}_2$.

It is clear from the discussion in the subsection that the estimation and tracking errors can asymptotically converge to zero as $t \longrightarrow \infty$ under the consensus algorithm (74).

4. Simulation Result

Some numerical simulations are to verify the effectiveness of the theoretical results proposed above in the section. The multi-UUVs system has five vehicles consisting of one UUV leader indexed by 0 and four UUV followers indexed by $1, 2, 3, 4$ under switching communication topology (Figure 3) with unmeasurable disturbances (98) using the consensus algorithm (74). We consider the nonlinear UUV model (1) and the double-integrator dynamic model (49) and (51), noting that the leader is independent of the following UUVs and sends the state information to the part of the followers, and the followers only exchange the position information state with their the local neighbours in the paper. The parameters of the nonlinear UUV model refer to [50]. These five UUVs are randomly located in the three-dimensional space of $[0, 50] \times [0, 30] \times [0, -10]$. The initial pitch and heave of the UUVs set $[-(\pi/18), \pi/18]$ and $[0, 2\pi]$, respectively. The original velocity of the UUVs is zero. The DESO is used to estimate the velocity information state and disturbances timely for each following UUV. The following disturbances

$$
\begin{aligned}
d_1 &= \begin{cases} 1 + 0.001e^{-0.001t}\sin((1/2)t)x_{1i}, & i = 1, \ldots 5,\ t < 15\,\text{s}, \\ -1 + 0.001e^{-0.001(t-15)}\sin((1/2)t)v_{1i}, & i = 1, \ldots 5, t \geq 15\,\text{s}, \end{cases} \\
d_2 &= \begin{cases} -2 - 0.0015e^{-0.0005t}\sin((1/2)t)x_{2i}, & i = 1, \ldots 5, t < 15\,\text{s}, \\ 2 + 0.0015e^{-0.0005(t-15)}\sin((1/2)t)v_{2i}, & i = 1, \ldots 5, t \geq 15\,\text{s}, \end{cases} \\
d_3 &= \begin{cases} -3 + 0.002e^{-0.002t}\sin((1/2)t)x_{3i}, & i = 1, \ldots 5, t < 15\,\text{s}, \\ 5 + 0.002e^{-0.002(t-15)}\sin((1/2)t)v_{3i}, & i = 1, \ldots 5, t \geq 15\,\text{s}, \end{cases} \\
d_4 &= \begin{cases} 4 - 0.0025e^{-0.001t}\sin((1/2)t)x_{4i}, & i = 1, \ldots, 5,\ t < 15\,\text{s}, \\ -4 - 0.0025e^{-0.001(t-15)}\sin((1/2)t)v_{4i}, & i = 1, \ldots, 5,\ t \geq 15\,\text{s}, \end{cases}
\end{aligned} \tag{98}
$$

are considered to be imposed on each UUV system.

For simplicity, we assume that the possible communication topology for these five UUVs are the set $\{\overline{G}_1, \overline{G}_2, \overline{G}_3, \overline{G}_4, \overline{G}_5, \overline{G}_6\}$ shown in Figure 3, and switches sequentially circularly from the set, namely, $\overline{G}_1 \longrightarrow \overline{G}_2 \longrightarrow \overline{G}_3 \longrightarrow \overline{G}_4 \longrightarrow \overline{G}_5 \longrightarrow \overline{G}_6 \longrightarrow \overline{G}_1 \longrightarrow \cdots$,

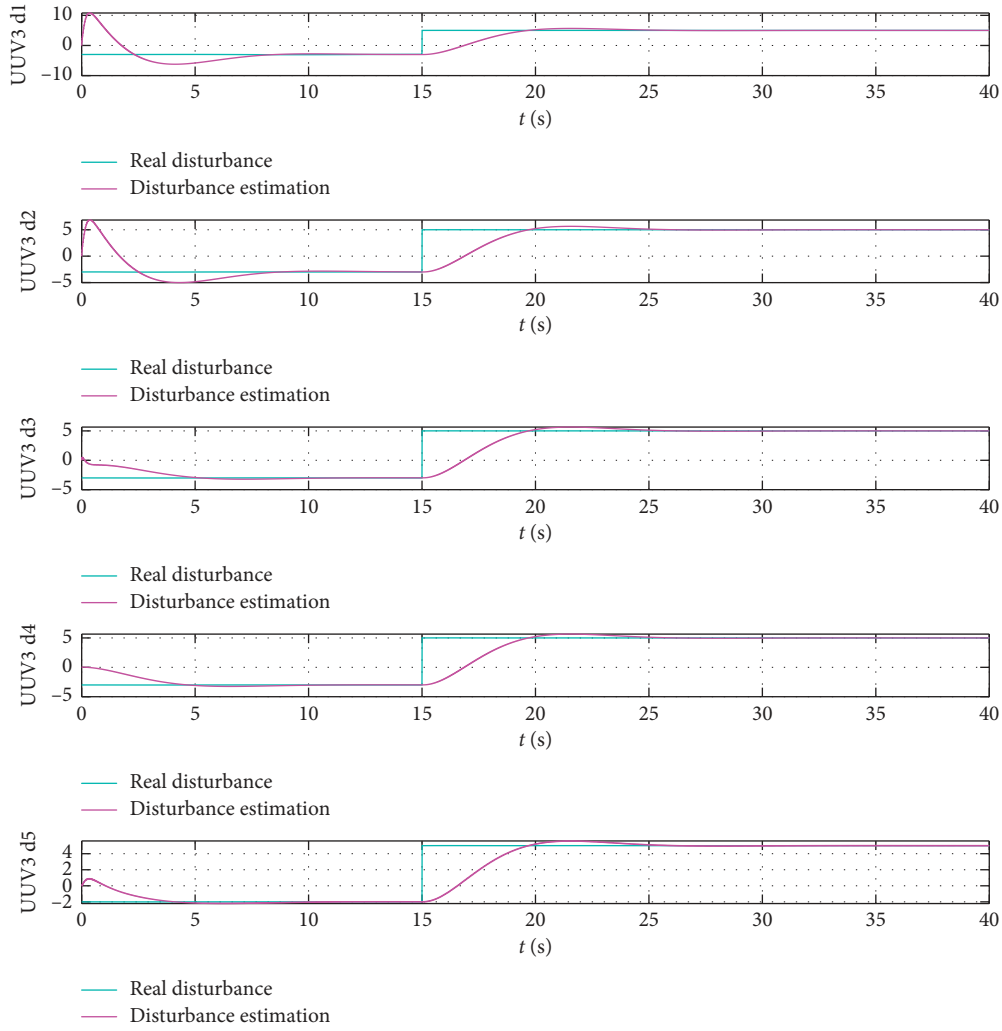

FIGURE 8: Comparison of real disturbance d_3 and disturbance estimation $\widehat{d}_3$.

and the dwell time of each graph is for 1/3 sec.. $\overline{G}_1 \cup \overline{G}_2 \cup \overline{G}_3$ and $\overline{G}_4 \cup \overline{G}_5 \cup \overline{G}_6$ are connected; then we can choose $t_k^0 = k$, $t_k^1 = k + (1/3)$, $t_k^2 = k + (2/3)$, $t_k^3 = k + 1$ with $k = 0, 1, \ldots$. According to Figure 3, we have the structure matrix F_i, $i = 1, \ldots, 6$ associated with $\overline{G}_i$, $i = 1, \ldots, 6$ and further obtain $\gamma_{\min} = 0.1981$. By solving (80) and (81), the solutions P_1 and P_2 are shown as follows:

$$P_1 = \begin{bmatrix} 0.8849 & -0.4741 & -0.3395 \\ -0.4741 & 0.8822 & -0.5373 \\ -0.3395 & -0.5373 & 2.0383 \end{bmatrix} \otimes I_{5\times5},$$
$$P_2 = \begin{bmatrix} 0.8543 & 0.8543 \\ 0.8543 & 2.5628 \end{bmatrix} \otimes I_{5\times5}. \tag{99}$$

According to Theorem 2, the observer gain E and the feedback control gain K are calculated as

$$E = \begin{bmatrix} -12.6367 \\ -9.6163 \\ -4.6397 \end{bmatrix} \otimes I_{5\times5},$$
$$K = \begin{bmatrix} -4.3125 & -12.9370 \end{bmatrix} \otimes I_{5\times5}. \tag{100}$$

Figure 4 shows the position and attitude states response curves of the leader-following multi-UUVs in presence of unmeasurable disturbances under the switching topology. It can be observed from the position figures x, y, and z that the following UUVs absolutely track the trajectory of the leader UUV. It is seen that the position and attitude states vary at 15 sec., since the changing lumped disturbances are added to each UUV system at 15 sec. The attitude figure θ indicates that the Euler angles θ of the following UUVs cannot completely converge to that of the leader UUV in presence of disturbances under the switching topologies, since the disturbances imposed on a multi-UUV system include the bounded function $\sin((1/2)t)$, which leads to estimation error converge to zero as time goes to infinity. However, the errors between the leader UUV and following UUVs are very small and within the allowable range, and the lumped disturbances can be attenuated according to the conclusion in the previous section, which means the consensus algorithm (74) can compensate for the disturbances in the UUV system.

Figure 5 presents the velocity states of the leader-following multi-UUVs system under the switching topology. As shown in the figure, the velocity state of each UUV can

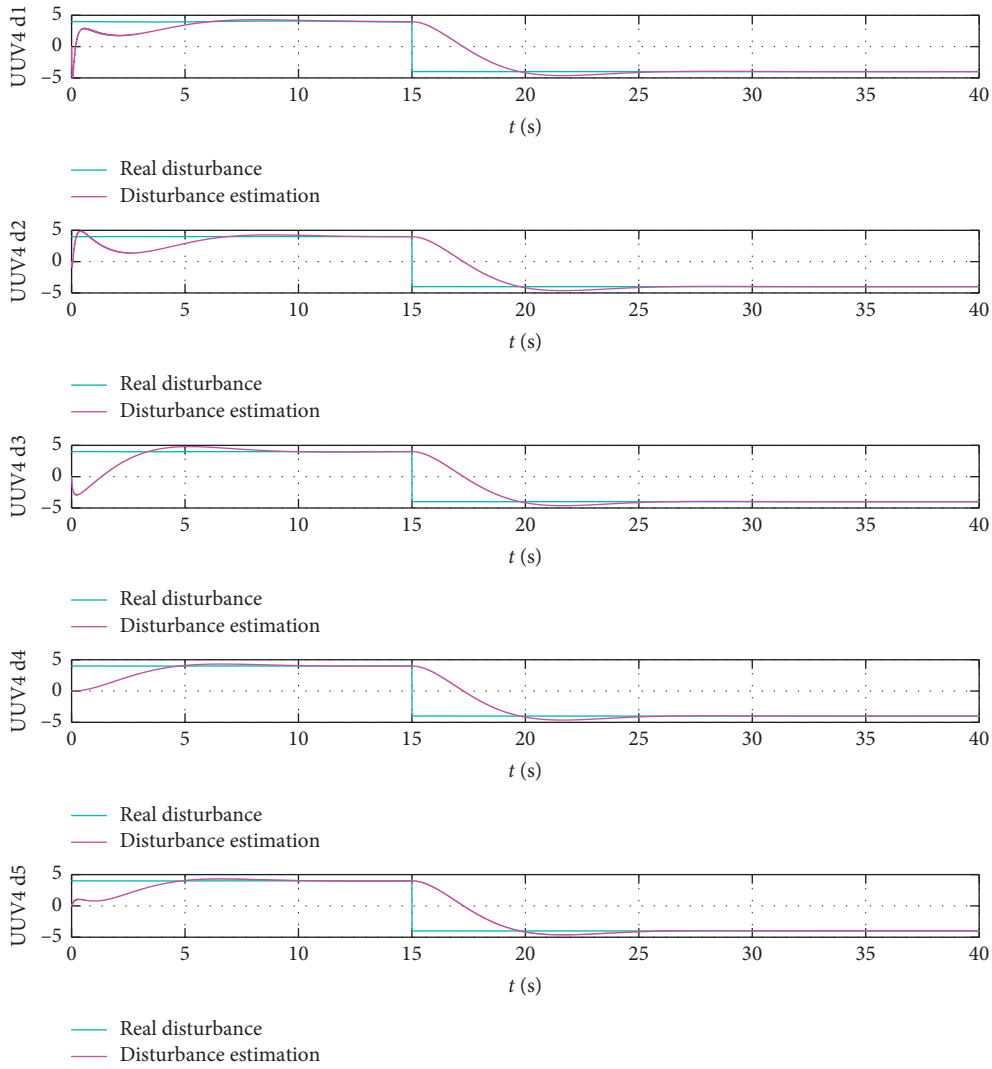

Figure 9: Comparison of real disturbance d_4 and disturbance estimation $\widehat{d}_4$.

follow that of leader UUV about 15 sec and then undergo changes because of imposing varying disturbances from 15 sec on the UUV system; however, the velocity state of each UUV finally converges that of the leader UUV.

From Figures 4 and 5, the leader-following multi-UUV system can reach consensus using the consensus algorithm (74) with unmeasurable disturbances under the switching topology.

The response curves of real disturbance and disturbance estimation for each UUV are shown in Figures 6–9. The disturbance d_i, $i = 1, 2, 3, 4$ acts on the UUV system over time. It can be observed from Figures 6–9 that DESO can estimate the changing lumped disturbances timely and the method proposed in the paper can obtain better disturbance rejection performance.

To illustrate the effectiveness of the algorithm proposed in the paper, the following consensus algorithm without considering the disturbance rejection for the multi-UUVs in [34] is employed for comparison. The feedback controller is shown as

$$u_i(t) = K \sum_{j \in N_i} a_{ij}\left(\widehat{\xi}_i - \widehat{\xi}_j\right) + q_i K\left(\widehat{\xi}_i - \xi_0\right). \tag{101}$$

To have a fair comparison, the switching topologies have the same structures shown in Figure 3. The gain K is taken the same as the previous derivation approach for K, where $K = -\varsigma B^T P$, $\varsigma \geq (1/\lambda_{\min}(F))$ and P is the symmetrical positive-define matrix solution to the following Riccati inequality:

$$A^T P + PA - 2PBB^T P < 0. \tag{102}$$

The gain K and symmetrical positive-define matrix P are $K = [-4.3125 \;\; 12.9370] \otimes I_{5\times5}$ and $P = \begin{bmatrix} 0.8543 & 0.8543 \\ 0.8543 & 2.5628 \end{bmatrix} \otimes I_{5\times5}$.

Figures 10 and 11 show the position and attitude states and the velocity states response curves under the algorithm (101) when there are disturbances (100) imposed on each UUV system. As shown in Figures 10 and 11, the leader-following consensus cannot be achieved for the multi-UUVs according to Definition 2. Especially, comparing with the

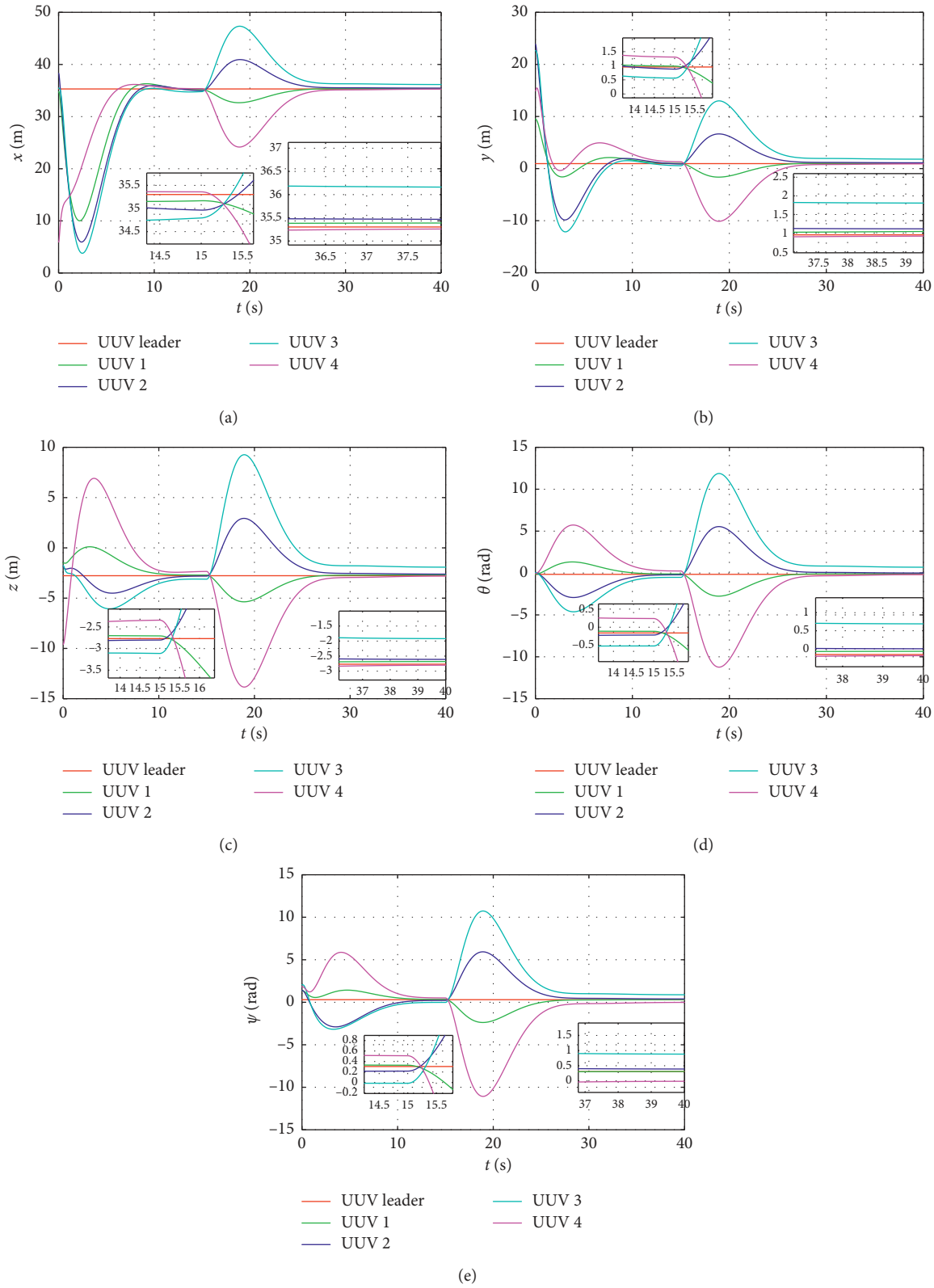

Figure 10: Position and attitude states of leader-following multi-UUVs with algorithm (101).

algorithm (74), the algorithm (101) cannot reach consensus control for multi-UUVs with disturbances under the switching topology before 15 sec. Note the proposed method (101) obtains poor control performance with big chattering in Figure 11. It is observed that the methods fail to reject the disturbances for multi-UUVs effectively.

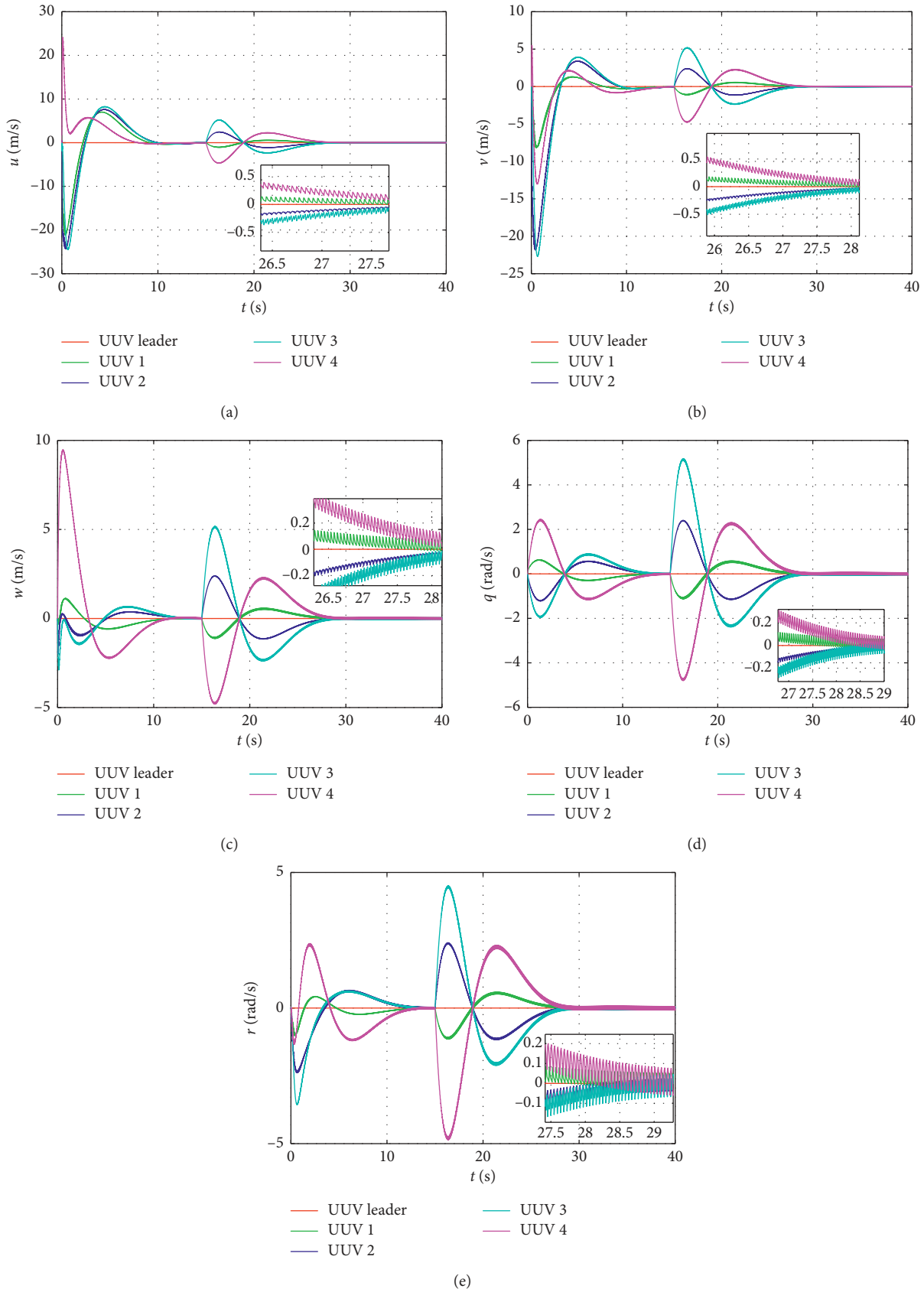

Figure 11: Velocity states of leader-following multi-UUVs with algorithm.

As compared with the algorithm (101), the proposed method in the paper has exhibited the superiority of rejecting the disturbances for multi-UUVs system under the switching topology.

5. Conclusion

The paper tackles the problems of tracking consensus problems with the disturbances under the fixed and switching topologies for the multi-UUVs system. A complex nonlinear and couple model of the UUV is transformed into a second-order integral UUV model by the method of the feedback linearization method. For the unmeasurable disturbance consisting of unknown model uncertainties and external disturbance for each UUV, we design DESO to estimate the disturbances utilizing the UUV position information relative to its neighbour UUVs. Moreover, leader-following multi-UUVs consensus control algorithm that enables all following UUVs to track the leader UUV state information based on the estimation state information from the DESO is proposed for two types of topologies, the fixed and switching topologies. Finally, simulation results are shown to demonstrate the multi-UUVs system in presence of unmeasurable disturbances under switching topologies can accomplish consensus control asymptotically.

Data Availability

The data used to support the findings of this study are available from the corresponding author upon request.

Conflicts of Interest

The authors declare no conflicts of interest.

Acknowledgments

This work was supported in part by the National Nature Science Foundation of China (grant 51679057/51709062), in part by Heilongjiang Province Outstanding Youth Fund (grant J2016JQ0052), in part by Equipment Preresearch Key Lab Fund (grant 614221580107), in part by China Postdoctoral Science Foundation (grant 2019M651265), and in part by Harbin Science and Technology Talent Research Special Fund (grant 2017RAQXJ150).

References

[1] B. Das, B. Subudhi, and B. B. Pati, "Cooperative formation control of autonomous underwater vehicles: an overview," *International Journal of Automation and Computing*, vol. 13, no. 3, pp. 199–225, 2016.

[2] X. Cao, H. B. Sun, and G. E. Jan, "Multi-AUV cooperative target search and tracking in unknown underwater environment," *Ocean Engineering*, vol. 150, pp. 1–11, 2018.

[3] X. Qi and Z.-j. Cai, "Three-dimensional formation control based on nonlinear small gain method for multiple underactuated underwater vehicles," *Ocean Engineering*, vol. 151, pp. 105–114, 2018.

[4] Z. Zhou, H. B. Wang, and Z. Q. Hu, "Event-based time varying formation control for multiple quadrotor UAVs with Markovian switching topologies," *Complexity*, vol. 2018, Article ID 8124861, 15 pages, 2018.

[5] K. Alam, T. Ray, and S. G. Anavatti, "Design optimization of an unmanned underwater vehicle using low- and high-fidelity models," *IEEE Transactions on Systems, Man, and Cybernetics: Systems*, vol. 47, no. 11, pp. 2794–2808, 2017.

[6] M. H. DeGroot, "Reaching a consensus," *Journal of the American Statistical Association*, vol. 69, no. 345, pp. 118–121, 1974.

[7] G. L. Gilardoni and M. K. Clayton, "On reaching a consensus using DeGroot's iterative pooling," *The Annals of Statistics*, vol. 21, no. 1, pp. 391–401, 1993.

[8] J. Tsitsiklis, D. Bertsekas, and M. Athans, "Distributed asynchronous deterministic and stochastic gradient optimization algorithms," *IEEE Transactions on Automatic Control*, vol. 31, no. 9, pp. 803–812, 1986.

[9] J. Hu and W. X. Zheng, "Adaptive tracking control of leader–follower systems with unknown dynamics and partial measurements," *Automatica*, vol. 50, no. 5, pp. 1416–1423, 2014.

[10] J. Hu, Y. Wu, T. Li, and B. K. Ghosh, "Consensus control of general linear multiagent systems with antagonistic interactions and communication noises," *IEEE Transactions on Automatic Control*, vol. 64, no. 5, pp. 2122–2127, 2019.

[11] S. Li and X. Wang, "Finite-time consensus and collision avoidance control algorithms for multiple AUVs," *Automatica*, vol. 49, no. 11, pp. 3359–3367, 2013.

[12] Z. Gao and G. Guo, "Fixed-time leader-follower formation control of autonomous underwater vehicles with event-triggered intermittent communications," *IEEE Access*, vol. 6, pp. 27902–27911, 2018.

[13] S. Chen and D. W. C. Ho, "Consensus control for multiple AUVs under imperfect information caused by communication faults," *Information Sciences*, vol. 370-371, pp. 565–577, 2016.

[14] T. Yang, S. Yu, and Y. Yan, "Formation control of multiple underwater vehicles subject to communication faults and uncertainties," *Applied Ocean Research*, vol. 82, pp. 109–116, 2019.

[15] B. Das, B. Subudhi, and B. B. Pati, "Employing nonlinear observer for formation control of AUVs under communication constraints," *International Journal of Intelligent Unmanned Systems*, vol. 3, no. 2-3, pp. 122–155, 2015.

[16] B. K. Sahu and B. Subudhi, "Flocking control of multiple AUVs based on fuzzy potential functions," *IEEE Transactions on Fuzzy Systems*, vol. 26, no. 5, pp. 2539–2551, 2018.

[17] D. Atta and B. Subudhi, "Decentralized formation control of multiple autonomous underwater vehicles," *International Journal of Robotics & Automation*, vol. 28, no. 4, pp. 303–310, 2013.

[18] M. Enayat and K. Khorasani, "Semi-decentralized nonlinear cooperative control strategies for a network of heterogeneous autonomous underwater vehicles," *International Journal of Robust and Nonlinear Control*, vol. 27, no. 16, pp. 2688–2707, 2017.

[19] Z. Yan, Y. Wu, X. Du, and J. Li, "Limited communication consensus control of leader-following multi-UUVs in a swarm system under multi-independent switching topologies and time delay," *IEEE Access*, vol. 6, pp. 33183–33200, 2018.

[20] Z. P. Yan, D. Wu, W. Zhang, and Y. B. Liu, "Consensus of multiagent systems with packet losses and communication delays using a novel control protocol," *Abstract and Applied Analysis*, vol. 2014, Article ID 159609, 13 pages, 2014.

[21] Z. P. Yan, Y. B. Liu, J. J. Zhou, W. Zhang, and L. Wang, "Consees of multiple autonomous underwater vehicles with

double independent Markovian switching topologies and timevarying delays," *Chinese Physics B*, vol. 26, no. 4, 2017.

[22] Z.-p. Yan, Y.-b. Liu, C.-b. Yu, and J.-j. Zhou, "Leader-following coordination of multiple UUVs formation under two independent topologies and time-varying delays," *Journal of Central South University*, vol. 24, no. 2, pp. 382–393, 2017.

[23] Z.-G. Wu, Y. Xu, Y.-J. Pan, H. Su, and Y. Tang, "Event-triggered control for consensus problem in multi-agent systems with quantized relative state measurements and external disturbance," *IEEE Transactions on Circuits and Systems I: Regular Papers*, vol. 65, no. 7, pp. 2232–2242, 2018.

[24] G. Ren and Y. Yu, "Robust consensus of fractional multi-agent systems with external disturbances," *Neurocomputing*, vol. 218, pp. 339–345, 2016.

[25] Y. Wu, Y. Zhao, and J. Hu, "Bipartite consensus control of high-order multiagent systems with unknown disturbances," *IEEE Transactions on Systems, Man, and Cybernetics: Systems*, vol. 49, no. 10, pp. 2189–2199, 2017.

[26] H. Liu, Y. Lyu, F. L. Lewis, and Y. Wan, "Robust time-varying formation control for multiple underwater vehicles subject to nonlinearities and uncertainties," *International Journal of Robust and Nonlinear Control*, vol. 29, no. 9, pp. 2712–2724, 2019.

[27] Z. P. Yan, D. Xu, T. Chen, W. Zhang, and Y. B. Liu, "Leader-follower formation control of UUVs with model uncertainties, current disturbances, and unstable communication," *Sensors*, vol. 18, no. 2, p. 662, 2018.

[28] G. Xia, C. Sun, B. Zhao, and J. Xue, "Cooperative control of multiple dynamic positioning vessels with input saturation based on finite-time disturbance observer," *International Journal of Control, Automation and Systems*, vol. 17, no. 2, pp. 370–379, 2019.

[29] Z. Peng, J. Wang, and J. Wang, "Constrained control of autonomous underwater vehicles based on command optimization and disturbance estimation," *IEEE Transactions on Industrial Electronics*, vol. 66, no. 5, pp. 3627–3635, 2019.

[30] X. Wang and G.-H. Yang, "Cooperative adaptive fault-tolerant tracking control for a class of multi-agent systems with actuator failures and mismatched parameter uncertainties," *IET Control Theory & Applications*, vol. 9, no. 8, pp. 1274–1284, 2015.

[31] X. Wang and G.-H. Yang, "Adaptive reliable coordination control for linear agent networks with intermittent communication constraints," *IEEE Transactions on Control of Network Systems*, vol. 5, no. 3, pp. 1120–1131, 2018.

[32] Y. Wu, Y. Zhao, and J. Hu, "Optimal output anti-synchronisation of cooperative-competitive multi-agent systems via distributed observer," *IET Control Theory & Applications*, vol. 13, no. 13, pp. 2029–2038, 2019.

[33] Y. T. Wang and Y. Yao, "Consensus path-following control of multiple underactuated unmanned underwater vehicles," *Complexity*, vol. 2018, Article ID 4975187, 8 pages, 2018.

[34] L. Qiao and W. Zhang, "Double-loop integral terminal sliding mode tracking control for UUVs with adaptive dynamic compensation of uncertainties and disturbances," *IEEE Journal of Oceanic Engineering*, vol. 44, no. 1, pp. 29–53, 2019.

[35] Y. T. Wang and Y. N. Zhang, "Coordinated depth control of multiple autonomous underwater vehicles by using theory of adaptive sliding mode," *Complexity*, vol. 2018, Article ID 4180275, 12 pages, 2018.

[36] L. Qiao and W. Zhang, "Adaptive non-singular integral terminal sliding mode tracking control for autonomous underwater vehicles," *IET Control Theory & Applications*, vol. 11, no. 8, pp. 1293–1306, 2017.

[37] L. Zhao, Y. Jia, and J. Yu, "Neutral networks-based adaptive fixed-time consensus tracking control for uncertain multiple AUVs," *Journal of Robotics, Networking and Artificial Life*, vol. 4, no. 3, pp. 179–182, 2017.

[38] C. Yuan, S. Licht, and H. He, "Formation learning control of multiple autonomous underwater vehicles with heterogeneous nonlinear uncertain dynamics," *IEEE Transactions on Cybernetics*, vol. 48, no. 10, pp. 2920–2934, 2018.

[39] G. Xia, C. Sun, B. Zhao, X. Xia, and X. Sun, "Neuroadaptive distributed output feedback tracking control for multiple Marine surface vessels with input and output constraints," *IEEE Access*, vol. 7, no. 1, pp. 123076–123085, 2019.

[40] K. Shojaei and M. M. Arefi, "On the neuro-adaptive feedback linearising control of underactuated autonomous underwater vehicles in three-dimensional space," *IET Control Theory & Applications*, vol. 9, no. 8, pp. 1264–1273, 2015.

[41] W. Cao, J. Zhang, and W. Ren, "Leader–follower consensus of linear multi-agent systems with unknown external disturbances," *Systems & Control Letters*, vol. 82, pp. 64–70, 2015.

[42] W. Ren and R. W. Beard, *Distributed Consensus in Multi-Vehicle Cooperative Control*, Springer, London, UK, 2008.

[43] T. I. Fossen, *Handbook of Marine Craft Hydrodynamics and Motion Control*, John Wiley & Sons, Hoboken, NJ, USA, 2011.

[44] H. K. Khalil and S. W. Shaw, *Stability Theory, Nonlinear. Wiley Encyclopedia of Electrical and Electronics Engineering*, John Wiley & Sons, Hoboken, NJ, USA, 1999.

[45] J. Q. Han, "The extended state observer of a class of uncertain system," *Control and Decision*, vol. 10, no. 1, pp. 85–88, Jan 1995.

[46] S. Li, J. Yang, W. H. Chen, and X. Chen, *Disturbance Observer-Based Control: Methods and Applications*, CRC Press, Inc., Boca Raton, FL, USA, 2014.

[47] S. Li, J. Yang, W.-H. Chen, and X. Chen, "Generalized extended state observer based control for systems with mismatched uncertainties," *IEEE Transactions on Industrial Electronics*, vol. 59, no. 12, pp. 4792–4802, 2012.

[48] A. Jadbabaie, J. Lin, and A. S. Morse, "Coordination of groups of mobile autonomous agents using nearest neighbor rules," *IEEE Transactions on Automatic Control*, vol. 48, no. 6, pp. 988–1001, 2003.

[49] Y. Hong, L. Gao, D. Cheng, and J. Hu, "Lyapunov-based approach to multiagent systems with switching jointly connected interconnection," *IEEE Transactions on Automatic Control*, vol. 52, no. 5, pp. 943–948, 2007.

[50] Z.-p. Yan, H.-m. Yu, and B.-y. Li, "Bottom-following control for an underactuated unmanned undersea vehicle using integral-terminal sliding mode control," *Journal of Central South University*, vol. 22, no. 11, pp. 4193–4204, 2015.